Revista Internacional de Métodos Numéricos para Cálculo y Diseño en Ingeniería

Tech Science Press

https://doi.org/10.32604/rimni.2026.073803

ARTICLE

Computational Analysis of the Jointly Type-I Hybrid Censoring Plan and Its Three Engineering Applications

Refah Alotaibi[1], Hoda Rezk[2] and Ahmed Elshahhat[3,*]

[1]Department of Mathematical Sciences, College of Science, Princess Nourah bint Abdulrahman University, P.O. Box 84428, Riyadh, 11671, Saudi Arabia

[2]Department of Statistics, Al-Azhar University, Cairo, 11884, Egypt

[3]Faculty of Technology and Development, Zagazig University, Zagazig, 44519, Egypt

*Corresponding Author: Ahmed Elshahhat. Email: aelshahhat@ftd.zu.edu.eg.

Received: 25 September 2025; Accepted: 05 December 2025; Published: 06 November 2026

ABSTRACT: Joint censoring mechanisms play a pivotal role in life-test comparison studies, particularly when assessing items manufactured across different production lines within the same organization. This work introduces a comprehensive inferential framework for analyzing jointly hybrid Type-I censored samples derived from two independent Nadarajah–Haghighi (NH) populations—a versatile lifetime distribution capable of modeling a wide spectrum of hazard behaviors beyond the exponential family. Parameter estimation for the NH model is carried out through maximum likelihood methods using Newton–Raphson iterations, with asymptotic confidence intervals constructed via logarithmic transformations to mitigate boundary complications. Complementing the frequentist approach, a Bayesian methodology is developed under independent gamma priors. Posterior inference is obtained through a Metropolis–Hastings algorithm, enabling efficient computation of Bayesian point estimates, credible intervals, and highest posterior density regions. The proposed methodology also integrates stochastic techniques to enhance reliability modeling and failure-time data analysis. To assess performance, extensive Monte Carlo experiments are conducted across varying sample sizes, censoring schemes, and prior settings. The practical utility of the methods is demonstrated through three engineering applications, where the proposed models successfully capture intricate reliability structures and provide valuable insights for product life-cycle management.

KEYWORDS: Joint censoring; Nadarajah-Haghighi; likelihood and Bayesian; reliability; engineering data modeling

1 Introduction

In modern reliability assessment, traditional full-duration testing is increasingly being replaced by more efficient methodologies that embrace incomplete failure observations. Particularly when evaluating highly durable systems, researchers often opt to terminate experiments before all units fail—an approach that not only conserves resources but also strategically retains units for subsequent investigations or redeployment. This paradigm shift has given rise to the widespread use of censored samples, where partial failure data forms the basis of inference. Such designs enable accelerated testing while maintaining inferential validity, aligning with the growing demand for time- and cost-efficient analysis in high-reliability engineering. In a Type-I censoring design, the experiment is stopped at a predetermined time $t^{\star}$, regardless of how many failures have occurred by that point.

In contrast, Type-II censoring concludes once a fixed number of failures, say m, has been observed, irrespective of the time taken to reach this count; see Balakrishnan and Kundu [1] for comprehensive

Copyright © 2027 The Authors. Published by Tech Science Press. This work is licensed under a Creative Commons Attribution 4.0 International License, which permits unrestricted use, distribution, and reproduction in any medium, provided the original work is properly cited.

treatment. To incorporate the advantages of both strategies, Epstein [2] introduced the Type-I hybrid censoring scheme, where the experiment terminates at $\min(t^\star, X_{m:n})$, with $X_{m:n}$ denoting the m-th order statistic of the failure times. While this hybrid approach offers practical flexibility, it may result in fewer than m observed failures, thus potentially limiting the inferential power of the data. To address this shortcoming, Childs et al. [3] proposed the Type-II hybrid censoring (T2-HC), in which the experiment is concluded at $\max(t^\star, X_{m:n})$. This ensures that at least m failure times are always observed, thereby enhancing the reliability of parameter estimation and overall inference. Consequently, the T2-HC design is generally regarded as more informative and statistically advantageous compared to its Type-I hybrid counterpart.

In recent years, joint censoring plans have received a lot of attention as effective tools for conducting comparative life testing across multiple manufacturing lines. These plans enable researchers to simultaneously monitor and analyze product reliability from multiple sources or production processes, allowing for efficient data collection and meaningful statistical inference. Several joint censoring frameworks have been introduced to address various experimental requirements and constraints. Particularly, Balakrishnan and Rasouli [4] proposed the joint Type-II censoring (JT2-C), while Su [5] introduced a joint Type-I hybrid censoring (JT1-HC). Further developments include the generalized JT1-HC by Su and Zhu [6]. In parallel, several joint multi-stage censoring designs have also been introduced. For example, Rasouli and Balakrishnan [7], and later Sultana et al. [8], proposed progressive JT2-C plan. In next section, our primary focus is on the JT1-HC strategy recently developed by Elshahhat et al. [9]. The proposed JT1-HC strategy provides a natural extension of classical single-population hybrid censoring schemes to a two-population comparative reliability framework. In many industrial experiments, it is often necessary to evaluate and compare the performance of products manufactured on different production lines under identical testing environments. Traditional single-sample censoring schemes cannot accommodate such comparative assessments efficiently, since they analyze each population separately, resulting in increased testing time and experimental cost. The JT1-HC plan, on the other hand, allows the two populations to be tested simultaneously under a unified censoring structure, enabling more economical data collection and providing richer inferential information. From a methodological viewpoint, the joint likelihood combines the failure information from both samples, thereby improving estimation precision and reducing the uncertainty associated with reliability comparisons.

The Nadarajah–Haghighi (NH) distribution, introduced by Nadarajah and Haghighi [10], is a flexible two-parameter lifetime model that has received growing attention in reliability and survival analysis. Unlike the exponential distribution, which imposes a restrictive assumption of a constant failure rate, the NH distribution accommodates a wider range of failure behaviors, such as decreasing, increasing, or constant forms. One of the key strengths of the NH distribution is its ability to outperform traditional models such as the exponential, gamma, or Weibull distributions in scenarios where those models fail to capture the underlying failure behavior effectively. An additional advantage of the NH distribution is its ability to model datasets that include zero values, a limitation often encountered with other lifetime models. Due to this versatility, the NH distribution has gained traction in the literature and is sometimes referred to as the extended exponential distribution. Subsequently, in recent years, the NH distribution has been successfully incorporated into various complex censoring schemes, further extending its utility in reliability studies; see, for example, Kumar et al. [11,12].

In applied settings, JT1-HC of two NH populations is especially useful when experimental costs or time limits prevent full lifetime observation, as in reliability testing or clinical trials. By handling censored data from both groups, this method provides more accurate reliability evaluations and strengthens the scientific credibility of comparative studies across various application fields. Let $\mathbb{X} = \{X_1, \ldots, X_{n_1}\}$ be the lifetimes of n_1 selected from population I which are independently and identically distributed (iid) random variables from the NH distribution, i.e., $\mathbb{X} \sim \text{NH}(\boldsymbol{\alpha}_1)$, where $\lambda_1 > 0$ and $\theta_1 > 0$ are the scale and

shape parameters, respectively. Therefore, the associated probability density function (PDF) and cumulative distribution function (CDF) of $\mathbb{X}$ can be expressed, respectively, as Eqs. (1) and (2):

$$g(x;\boldsymbol{\alpha}_1) = \theta_1\lambda_1(1+\lambda_1 x)^{\theta_1-1}\exp(1-(1+\lambda_1 x)^{\theta_1}),\ x>0, \tag{1}$$

and

$$G(x;\boldsymbol{\alpha}_1) = 1-\exp(1-(1+\lambda_1 x)^{\theta_1}), \tag{2}$$

where $\boldsymbol{\alpha}_1 = (\theta_1,\lambda_1)^\top$. In a similar way, we suppose the lifetimes $\mathbb{Y} = \{Y_1,\ldots,Y_{n_2}\}$ selected from population II are iid random variables, where $\mathbb{Y} \sim \mathrm{NH}(\boldsymbol{\alpha}_2)$, where $\lambda_2 > 0$ and $\theta_2 > 0$ are the scale and shape parameters, respectively. Therefore, where $\boldsymbol{\alpha}_2 = (\theta_2,\lambda_2)^\top$, the associated PDF and CDF of $\mathbb{Y}$ can be expressed, respectively, as Eqs. (3) and (4):

$$g(y;\boldsymbol{\alpha}_2) = \theta_2\lambda_2(1+\lambda_2 y)^{\theta_2-1}\exp(1-(1+\lambda_2 y)^{\theta_2}),\ y>0, \tag{3}$$

and

$$G(y;\boldsymbol{\alpha}_2) = 1-\exp(1-(1+\lambda_2 y)^{\theta_2}). \tag{4}$$

Numerous studies have explored parameter estimation for the NH distribution under various censoring schemes. Researchers have proposed methods for handling different forms of incomplete data, including progressively first-failure (by Ashour et al. [13]), progressive Type-I and Type-II (by Elbatal et al. [14] and Wu and Gui [15], respectively), Type-I generalized progressively hybrid (by Elshahhat and Abu El Azm [16]), constant-stress partially accelerated tests (by Dey et al. [17]), Type-I and Type-II adaptive progressively hybrid (by Almarashi et al. [18] and Elshahhat et al. [19], respectively), joint Type-II progressive (by Hasaballah et al. [20]), and improved adaptive Type-II progressive (by El-Sherpieny et al. [21]). Collectively, these contributions highlight the flexibility of the NH distribution in accommodating complex censoring structures in reliability analysis.

The motivation for adopting the JT1-HC design lies in its ability to balance statistical efficiency with experimental practicality. Unlike the JT2-HC plan, which enforces continuation until a fixed number of failures are observed, the JT1-HC plan permits early termination at a predetermined time threshold while still ensuring adequate data for inference. This property is especially valuable in industrial life-testing contexts where time or safety limitations make extended testing undesirable. Moreover, compared with more generalized or multi-stage censoring frameworks, the JT1-HC structure maintains analytical simplicity and computational stability, particularly in the context of Bayesian inference, without significant loss of inferential precision. Hence, the proposed joint framework under the JT1-HC design achieves a favorable compromise between flexibility, interpretability, and computational feasibility.

The main contributions of this study can be outlined as follows:

- This work combines the JT1-HC plan with the NH populations, offering a new framework that can handle more flexible lifetime behaviors while keeping experiments efficient.
- The maximum likelihood estimators (MLEs) of the NH parameters under JT1-HC are derived, and the corresponding asymptotic confidence intervals (ACIs) are constructed, with log-transform methods applied to prevent negative or unrealistic bounds.
- A Bayesian approach is proposed using independent gamma priors, and the Metropolis–Hastings algorithm is employed to obtain Bayes estimates, credible intervals, and highest posterior density (HPD) regions.

- An extensive Monte Carlo study is carried out to check how the proposed methods perform under different sample sizes, censoring levels, and prior settings.
- The simulation results show that Bayesian methods, especially with informative priors, generally perform better than the frequentist approach, giving smaller biases, lower mean squared errors, and more reliable interval estimates.
- The proposed methodology is applied to failure times in three benchmark datasets, namely capacity factor, mechanical equipment failures, and air-conditioning systems. These applications demonstrate the practical usefulness of the approach in modeling complex real-world reliability phenomena.

The remainder of the paper is organized as follows: Section 2 introduces the proposed scheme, while Sections 3 and 4 present the classical and Bayesian estimation procedures of the model parameters, respectively. Section 5 reports the results of simulation studies, and Section 6 illustrates three engineering applications. Finally, Section 7 provides concluding remarks.

2 JT1-HC Plan

The JT1-HC plan can be formally described as follows: Suppose two items, denoted by A and B, are manufactured in the same facility but originate from two distinct production lines, labeled L_1 and L_2, respectively. Let $\mathbb{X} = \{X_1, X_2, \ldots, X_{n_1}\}$ and $\mathbb{Y} = \{Y_1, Y_2, \ldots, Y_{n_2}\}$ represent two independent samples of sizes n_1 and n_2, corresponding to items A and B placed simultaneously under life testing.

The total number of units under examination is $n^\star = \sum_{i=1}^{2} n_i$. It is assumed that the lifetimes in $\mathbb{X}$ ($\mathbb{Y}$) are iid with CDF $G_X(\cdot)$ ($G_Y(\cdot)$) and with PDF $g_X(\cdot)$ ($g_Y(\cdot)$). Based on prior manufacturing or operational constraints, a termination threshold time $t^\star$ is specified in advance. Let $W_{(1)} \le W_{(2)} \le \cdots \le W_{(n^\star)}$ denote the order statistics of the lifetimes from $\{\mathbb{X}; \mathbb{Y}\} = \{X_1, \ldots, X_{n_1}; Y_1, \ldots, Y_{n_2}\}$. Let m be the desired number of observed failed units. To reduce experimental cost and duration, the investigator employs the proposed JT1-HC scheme. Hence, the observed data are denoted by $(\mathbf{w}, \boldsymbol{\zeta})$ and take one of the following forms:

$$(\mathbf{w}, \boldsymbol{\zeta}) = \begin{cases} \{w_{(1)}, w_{(2)}, \ldots, w_{(m)}; \zeta_1, \zeta_2, \ldots, \zeta_m\}, & \text{if } w_{(m)} \le t^\star \quad \text{(Case 1)}; \\ \{w_{(1)}, w_{(2)}, \ldots, w_{(d)}; \zeta_1, \zeta_2, \ldots, \zeta_d\}, & \text{if } w_{(m)} > t^\star \quad \text{(Case 2)}. \end{cases}$$

Here, d denotes the number of failures observed before reaching the censoring time $t^\star$. Let $n_1^\bullet = \sum_{i=1}^{\mathcal{D}^\star} \zeta_i$ and $n_2^\bullet = \sum_{i=1}^{\mathcal{D}^\star} (1 - \zeta_i)$ denote the number of observed failures from samples $\mathbb{X}$ and $\mathbb{Y}$, respectively, where $\mathcal{D}^\star = \sum_{i=1}^{2} n_i^\bullet$ represents the total number of failures, with $\mathcal{D}^\star \in \{1, 2, \ldots, n^\star\}$ indicating the effective sample size. A key advantage of the JT1-HC lies in its flexibility: the life-testing experiment terminates either after observing a pre-specified number of failures (m) or upon reaching the predetermined threshold time ($t^\star$), whichever occurs first. This dual stopping criterion provides a balance between data informativeness and resource efficiency. If the JT1-HC failure times of $n^\star$ specimens are coming from two independent samples of continuous population with PDFs $g(x; \boldsymbol{\alpha}_1)$ and $g(y; \boldsymbol{\alpha}_2)$, respectively, and the corresponding CDFs $G(x; \boldsymbol{\alpha}_1)$ and $G(y; \boldsymbol{\alpha}_2)$, respectively. Then, the joint PDF of $\boldsymbol{\alpha} = (\boldsymbol{\alpha}_1, \boldsymbol{\alpha}_2)^\top$ given $\mathbf{w}$ can be expressed as shown in Eq. (5):

$$L(\boldsymbol{\theta} | \mathbf{w}) \propto \prod_{i=1}^{\mathcal{D}^\star} [g(w_{(i)}; \boldsymbol{\alpha}_1)]^{\zeta_i} [g(w_{(i)}; \boldsymbol{\alpha}_2)]^{1-\zeta_i} [1 - G(\mathcal{T}^\star; \boldsymbol{\alpha}_1)]^{n_1^\star} [1 - G(\mathcal{T}^\star; \boldsymbol{\alpha}_2)]^{n_2^\star}, \tag{5}$$

where $n_i^\star = n_i - n_i^\bullet$, $i = 1, 2$,

$$\zeta_i = \begin{cases} 1, & \text{if } w_{(i)} \in \mathbb{X}; \\ 0, & \text{if } w_{(i)} \in \mathbb{Y}, \end{cases} \quad \text{and} \quad \mathcal{T}^\star = \begin{cases} m, & \text{if } w_{(i)} \in \mathbb{X}; \\ t^\star, & \text{if } w_{(i)} \in \mathbb{Y}. \end{cases}$$

It is worth noting that, from Eq. (5), when the threshold time $t^\star \to \infty$ and the pre-specified number of failures $m = n^\star$, the JT1-HC plan (by Su [5]) reduces to the JT2-C plan (by Balakrishnan and Rasouli [4]).

3 Classical Inference

In the case of such suggested censored data, this section displays presents the classical estimation of the model parameters θ_i and λ_i $(i = 1, 2)$, namely MLEs and ACIs of two independent NH population.

3.1 Estimators of Maximum Likelihood

Assuming that the lifetimes $\mathbb{X}$ (of size n_1 from facility-line L_1) are iid random variables from a NH$(\boldsymbol{\alpha}_1)$ population where λ_1 and θ_1 are the scale and shape parameters, respectively, with PDF and CDF in Eqs. (1) and (2) while let $\mathbb{Y}$ (of size n_2 from facility-line L_2) be iid random variables from another NH$(\boldsymbol{\alpha}_2)$ population where λ_2 and θ_2 are the scale and shape parameters, respectively, with PDF and CDF in Eqs. (3) and (4). The likelihood PDF (as shown in Eq. (6)) of $\boldsymbol{\alpha} = (\theta_1, \theta_2, \lambda_1, \lambda_2)^\top$ can be expressed proportionally as

$$\begin{aligned} L(\boldsymbol{\alpha} \mid w) \propto{}& (\theta_1\lambda_1)^{n_1^\bullet}(\theta_2\lambda_2)^{n_2^\bullet}\prod_{i=1}^{D^\star} A_1(w_i)A_2(w_i) \\ &\times \exp\left(\sum_{i=1}^{n_1^\bullet}(1 - A_1(w_i)) + \sum_{i=1}^{n_2^\bullet}(1 - A_2(w_i)) + n_1^\bullet(1 - A_1(\mathcal{T}^\star)) + n_2^\bullet(1 - A_2(\mathcal{T}^\star))\right), \end{aligned} \tag{6}$$

where $A_1(w_i) = (1 + \lambda_1 w_i)^{\theta_1 - 1}$ and $A_2(w_i) = (1 + \lambda_2 w_i)^{\theta_2 - 1}$.

From (6), the log-likelihood function as shown in Eq. (7), symbolized by $L^\star(\cdot) \propto \log L(\cdot)$, turns into

$$\begin{aligned} L^\star(\boldsymbol{\alpha} \mid w) \propto{}& n_1^\bullet \log(\theta_1\lambda_1) + n_2^\bullet \log(\theta_2\lambda_2) + \sum_{i=1}^{D^\star}\log(A_1(w_i)) + \sum_{i=1}^{D^\star}\log(A_2(w_i)) \\ &+ \sum_{i=1}^{n_1^\bullet}(1 - A_1(w_i)) + \sum_{i=1}^{n_2^\bullet}(1 - A_2(w_i)) + n_1^\bullet(1 - A_1(\mathcal{T}^\star)) + n_2^\bullet(1 - A_2(\mathcal{T}^\star)). \end{aligned} \tag{7}$$

Thus, the MLEs of (θ_1, λ_1) and (θ_2, λ_2), denoted by $(\hat{\theta}_1, \hat{\lambda}_1)$ and $(\hat{\theta}_2, \hat{\lambda}_2)$, are obtained by maximizing the log-likelihood function in Eq. (7). As shown in Eqs. (8)–(11), we derive the normal equations by setting the first-order partial derivatives of Eq. (7) with respect to (θ_i, λ_i) (for $i = 1, 2$) equal to zero, which yields:

$$\frac{\partial L^\star}{\partial \theta_1} = \frac{n_1^\bullet}{\theta_1} + \sum_{i=1}^{D^\star}\log(1 + \lambda_1 w_i) - \sum_{i=1}^{n_1^\bullet} A_1(w_i)\log(1 + \lambda_1 w_i) - n_1^\bullet A_1(\mathcal{T}^\star)\log(1 + \lambda_1 \mathcal{T}^\star), \tag{8}$$

$$\frac{\partial L^\star}{\partial \theta_2} = \frac{n_2^\bullet}{\theta_2} + \sum_{i=1}^{D^\star}\log\big(1 + \lambda_2 w_i\big) - \sum_{i=1}^{n_2^\bullet} A_2^\circ(w_i)\log\big(1 + \lambda_2 w_i\big) - n_2^\bullet A_2^\circ(\mathcal{T}^\star)\log\big(1 + \lambda_2 \mathcal{T}^\star\big), \tag{9}$$

$$\frac{\partial L^\star}{\partial \lambda_1} = \frac{n_1^\bullet}{\lambda_1} + (\theta_1 - 1)\sum_{i=1}^{D^\star}\frac{w_i}{1 + \lambda_1 w_i} - (\theta_1 - 1)\sum_{i=1}^{n_1^\bullet} w_i A_1^\circ(w_i) - n_1^\bullet(\theta_1 - 1)\mathcal{T}^\star A_1^\circ(\mathcal{T}^\star), \tag{10}$$

and

$$\frac{\partial L^\star}{\partial \lambda_2} = \frac{n_2^\bullet}{\lambda_2} + (\theta_2 - 1)\sum_{i=1}^{D^\star}\frac{w_i}{1 + \lambda_2 w_i} - (\theta_2 - 1)\sum_{i=1}^{n_2^\bullet} w_i A_2^\circ(w_i) - n_2^\bullet(\theta_2 - 1)\,\mathcal{T}^\star A_2^\circ(\mathcal{T}^\star), \tag{11}$$

where $A_1^{\circ}(w_i) = (1+\lambda_1 w_i)^{\theta_1-2}$ and $A_2^{\circ}(w_i) = (1+\lambda_2 w_i)^{\theta_2-2}$.

It is evident from Eqs. (8)–(11) that the estimators $(\hat{\theta}_i, \hat{\lambda}_i)$ (for $i = 1, 2$) cannot be obtained in closed form from a linear system of equations. To compute the MLE estimates, we recommend using the Newton–Raphson (NR) iterative algorithm. This algorithm exhibits rapid convergence for smooth log-likelihood functions, allowing it to quickly find highly accurate solutions, particularly when the initial guess is well-chosen. In practice, this algorithm can be conveniently implemented using the maxNR optimization routine available in the maxLik package (proposed by Henningsen and Toomet [22]) in R (version 4.2.2) programming environment, which numerically maximizes the objective functions in Eqs. (8)–(11) with respect to (θ_1, λ_1) and (θ_2, λ_2).

3.2 Estimators of Asymptotic Intervals

In addition to obtaining the frequentist point estimators, constructing two-sided $(1-\mu)100\%$ ACIs for $\boldsymbol{\alpha} = (\theta_1, \theta_2, \lambda_1, \lambda_2)^{\top}$ is of central importance. To this end, we rely on the asymptotic distributional properties of the MLEs $(\hat{\theta}_i, \hat{\lambda}_i)$ (for $i = 1, 2$). Specifically, under standard large-sample theory, the joint distribution of $\hat{\boldsymbol{\alpha}}^{\top}$ is approximately multivariate normal with mean vector $\boldsymbol{\alpha}$ and variance–covariance (V-Cov) matrix $\Psi(\alpha)$, where $\Psi(\cdot)$ is the inverse of the Fisher information (FI) matrix, $\Psi^{-1}(\cdot)$. However, deriving the exact closed-form of the FI matrix is analytically intractable owing to the nonlinear structure of its elements. Consequently, we employ the observed FI (OFI) matrix as a practical alternative, thereby obtaining the empirical estimate of the 4×4 V-Cov matrix (as defined in Eq. (12)) at $\boldsymbol{\alpha} = \hat{\boldsymbol{\alpha}}$; see, for more details Lawless [23], as expressed in Eq. (13):

$$\Psi^{-1}(\hat{\boldsymbol{\alpha}}) = -\begin{bmatrix} \mathcal{L}_{11} & & & \\ 0 & \mathcal{L}_{22} & & \\ \mathcal{L}_{31} & 0 & \mathcal{L}_{33} & \\ 0 & \mathcal{L}_{42} & 0 & \mathcal{L}_{44} \end{bmatrix}^{-1} \tag{12}$$

hence,

$$\Psi^{-1}(\hat{\boldsymbol{\alpha}}) = \begin{bmatrix} \operatorname{var}(\theta_1) & & & \\ 0 & \operatorname{var}(\theta_2) & & \\ \operatorname{cov}(\theta_1, \lambda_1) & 0 & \operatorname{var}(\lambda_1) & \\ 0 & \operatorname{cov}(\theta_2, \lambda_2) & 0 & \operatorname{var}(\lambda_2) \end{bmatrix}_{(\boldsymbol{\alpha}=\hat{\boldsymbol{\alpha}})}, \tag{13}$$

where $\hat{\boldsymbol{\alpha}} = (\hat{\theta}_1, \hat{\theta}_2, \hat{\lambda}_1, \hat{\lambda}_2)^{\top}$. All OFI items $\mathcal{L}_{ij}$ (for $i, j = 1, 2, 3, 4$) in Eqs. (A1)–(A6) are provided in Appendix A.

Then, at a $100(1-\mu)\%$ nominal confidence percentage, the corresponding $100(1-\mu)\%$ ACI estimator from the normality approximation approach (ACI-NA) for (θ_1, λ_1), can be expressed as shown in Eq. (14):

$$\hat{\theta}_1 \pm z_{0.5\mu}\sqrt{\widehat{\operatorname{var}}(\hat{\theta}_1)}, \quad \text{and} \quad \hat{\lambda}_1 \pm z_{0.5\mu}\sqrt{\widehat{\operatorname{var}}(\hat{\lambda}_1)}, \tag{14}$$

respectively, where $z_{0.5\mu}$ represents the upper $0.5\,\mu$-th quantile of the standard Gaussian distribution. Similarly, the $100(1-\mu)\%$ ACI-NA estimators for (θ_2, λ_2) can be easily developed.

It is worth noting that a well-known drawback of the conventional ACI-NA is its tendency to produce negative lower limits when applied to lifetime parameters, which is conceptually inappropriate in reliability analysis. To address this issue, researchers often replace negative lower bounds with zero.

To address this issue, Meeker and Escobar [24] advocated applying a logarithmic transformation to the MLEs prior to interval construction. Their investigations demonstrated that, among the alternative normal-based approaches, the ACI log-transformed-based (ACI-NL) provides superior coverage performance in most situations. For example, the $100(1-\mu)\%$ ACI-NL for the parameters (θ_1, λ_1) can be expressed as shown in Eq. (15):

$$\hat{\theta}_1 \times \exp\left(\pm z_{0.5\mu}\hat{\theta}_1^{-1}\sqrt{\widehat{\mathrm{var}}(\hat{\theta}_1)}\right) \quad \text{and} \quad \hat{\lambda}_1 \times \exp\left(\pm z_{0.5\mu}\hat{\lambda}_1^{-1}\sqrt{\widehat{\mathrm{var}}(\hat{\lambda}_1)}\right), \tag{15}$$

respectively. In a similar manner, the $100(1-\mu)\%$ ACI-NL estimators for (θ_2, λ_2) can be obtained directly.

4 Bayesian Inference

Within the Bayesian framework, prior knowledge and expert judgment can be systematically incorporated into the inferential process for model parameters. In this setting, the parameters α and ξ of the APE lifetime distribution are regarded as random quantities rather than fixed constants, and their prior distributions are chosen to reflect any available prior evidence. A natural and widely adopted option is to employ gamma priors, owing to their analytical tractability and flexibility, as highlighted in Kundu [25]. The gamma family is particularly appealing since it can represent a broad range of prior beliefs, from vague to highly informative specifications. It was also selected for Bayesian inference due to its conjugate flexibility for positive parameters and its ability to represent both informative and non-informative prior structures. For the Bayes' analysis, we assume that (θ_i, λ_i) (for $i = 1, 2$) are independent and distributed according to $\vartheta_s \sim \mathrm{Gamma}(a_{ij}, b_{ij})$, $i, j = 1, 2$, $s = 1, 2, 3, 4$, where $(\vartheta_1, \vartheta_2, \vartheta_3, \vartheta_4) = (\theta_1, \lambda_1, \theta_2, \lambda_2)$ the hyperparameters $a_{ii}, b_{ii} > 0$ $(i = 1, 2)$ are selected to encode prior information about the two independent $\mathrm{NH}(\boldsymbol{\alpha}_i)$ (for $i = 1, 2$) populations. Making use of this independence assumption, the joint prior PDF (as defined in Eq. (16)), say $\omega(\cdot)$, for (θ_i, λ_i) (for $i = 1, 2$) is given by

$$\omega(\boldsymbol{\alpha}) \propto \prod_{s=1}^{4} \vartheta_s^{a_{ij}-1} e^{-b_{ij}\vartheta_s}, \ i, j = 1, 2, \ s = 1, 2, 3, 4. \tag{16}$$

In Bayesian analysis, the posterior distribution represents the updated knowledge about the unknown parameters after combining prior information with the observed data. It is obtained by multiplying the likelihood function, which reflects how probable the observed data are for different parameter values, with the prior distribution, which encodes previous knowledge or expert opinion. In this study, the posterior distribution of the NH parameters (θ_i, λ_i) (for $i = 1, 2$), say $P(\cdot)$, can be expressed by combining Eqs. (6) and (16) as defined in Eq. (17):

$$\begin{aligned} P(\boldsymbol{\alpha} \mid w) \propto\ & \theta_1^{n_1^{\bullet}+a_{11}-1}\theta_2^{n_2^{\bullet}+a_{22}-1}\lambda_1^{n_1^{\bullet}+a_{12}-1}\lambda_2^{n_2^{\bullet}+a_{21}-1}e^{-[b_{11}\theta_1+b_{22}\theta_2+b_{12}\lambda_1+b_{21}\lambda_2]}\prod_{i=1}^{D^{\star}} A_1(w_i)A_2(w_i) \\ & \times \exp\left(\sum_{i=1}^{n_1^{\bullet}}(1-A_1(w_i)) + \sum_{i=1}^{n_2^{\bullet}}(1-A_2(w_i)) + n_1^{\bullet}(1-A_1(\mathcal{T}^{\star})) + n_2^{\bullet}(1-A_2(\mathcal{T}^{\star}))\right), \end{aligned} \tag{17}$$

where the associated normalized term (see Eq. (18)), say $\mathfrak{I}$, is given by

$$\mathfrak{I} = \int_{\theta_1}\int_{\theta_2}\int_{\lambda_1}\int_{\lambda_2} \omega(\boldsymbol{\alpha}) \times L(\boldsymbol{\alpha} \mid w)\, \mathrm{d}\theta_1\mathrm{d}\theta_2\mathrm{d}\lambda_1\mathrm{d}\lambda_2. \tag{18}$$

Now, as shown in Eq. (19), the Bayes estimator for any unknown parameter of θ_i or λ_i (for $i = 1, 2$), say $\tilde{v}(\boldsymbol{\alpha})$, is given by:

$$\tilde{v}(\boldsymbol{\alpha}) = \Im^{-1} \int_0^\infty \int_0^\infty \int_0^\infty \int_0^\infty v(\boldsymbol{\alpha}) P(\boldsymbol{\alpha} \mid w)\, \mathrm{d}\theta_1 \mathrm{d}\theta_2 \mathrm{d}\lambda_1 \mathrm{d}\lambda_2. \tag{19}$$

Since the ratio of integrals in Eq. (19) does not admit a closed-form solution, alternative computational approaches are required to obtain the Bayes estimates. One effective strategy is to employ the Markov chain Monte Carlo (MCMC) setup, which allows sampling from the posterior distribution and subsequently computing both the Bayes estimates and the corresponding BCI estimators.

Before going to generating MCMC samples, it is necessary to derive the conditional posterior distributions of $\theta_1,\ \theta_2,\ \lambda_1,\ \lambda_2$, based on Eq. (17), are given by Eqs. (20) and (21):

$$P_{\theta_1}(\theta_1|\boldsymbol{\alpha}_{-\theta_1}, w) \propto \theta_1^{n_1^\bullet + a_{11} - 1} e^{-b_{11}\theta_1} \exp\left(\sum_{i=1}^{n_1^\bullet} (1 - A_1(w_i)) + n_1^\bullet (1 - A_1(\mathcal{T}^\star))\right) \prod_{i=1}^{D^\star} A_1(w_i), \tag{20}$$

$$P_{\theta_2}(\theta_2|\boldsymbol{\alpha}_{-\theta_2}, w) \propto \theta_2^{n_2^\bullet + a_{22} - 1} e^{-b_{22}\theta_2} \exp\left(\sum_{i=1}^{n_2^\bullet} (1 - A_2(w_i)) + n_2^\bullet (1 - A_2(\mathcal{T}^\star))\right) \prod_{i=1}^{D^\star} A_2(w_i), \tag{21}$$

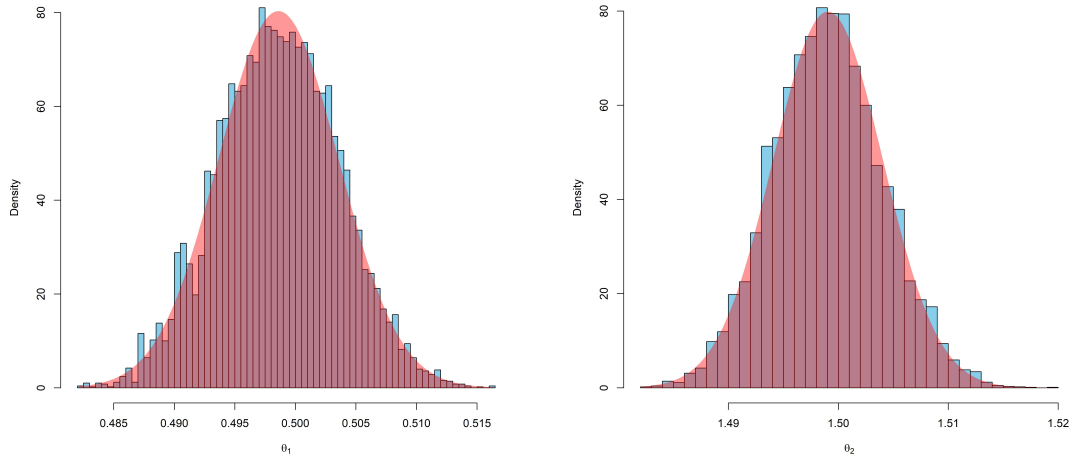
$$P_{\lambda_1}(\lambda_1|\boldsymbol{\alpha}_{-\lambda_1}, w) \propto \lambda_1^{n_1^\bullet + a_{12} - 1} e^{-b_{12}\lambda_1} \exp\left(\sum_{i=1}^{n_1^\bullet} (1 - A_1(w_i)) + n_1^\bullet (1 - A_1(\mathcal{T}^\star)) +\right) \prod_{i=1}^{D^\star} A_1(w_i), \tag{22}$$

and

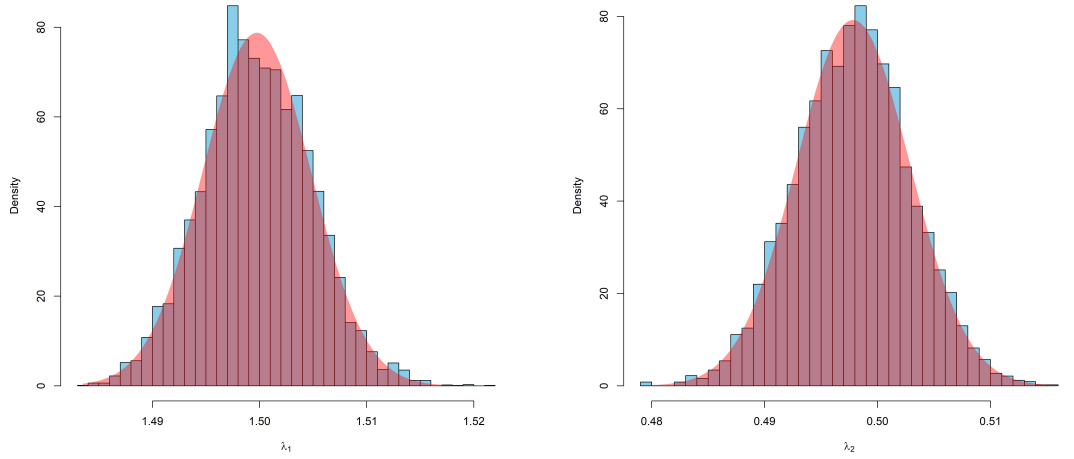
$$P_{\lambda_2}(\lambda_2|\boldsymbol{\alpha}_{-\lambda_2}, w) \propto \lambda_2^{n_2^\bullet + a_{21} - 1} e^{-b_{21}\lambda_2} \exp\left(\sum_{i=1}^{n_2^\bullet} (1 - A_2(w_i)) + n_2^\bullet (1 - A_2(\mathcal{T}^\star))\right) \prod_{i=1}^{D^\star} A_2(w_i), \tag{23}$$

respectively.

From Eqs. (20)–(23), it is clear that the full conditional posteriors of (θ_i, λ_i) (for $i = 1, 2$) do not correspond to any standard statistical model. Consequently, direct sampling from these conditionals using conventional techniques is not feasible. To overcome this limitation, we employ the Metropolis–Hastings (M-H) algorithm, which performs well in low-dimensional parameter settings and does not require closed-form full conditionals, ensuring stable and efficient convergence of the Bayesian estimates. Examination of the shapes in Eqs. (20)–(23) (see Fig. 1) indicates that they closely resemble normal distributions; hence, we adopt the normal distribution as the proposal density to generate candidate values. To generate posterior samples of (θ_i, λ_i) (for $i = 1, 2$) from their conditionals Eqs. (20)–(23), and subsequently compute their Bayes point estimates and credible intervals, do the procedure steps reported in Algorithm 1.



(a) θ_1 (b) θ_2



(c) λ_1 (d) λ_2

Figure 1: The posterior PDFs of (θ_i, λ_i) (for $i = 1, 2$).

Algorithm 1: The M-H sampling of (θ_i, λ_i) (for $i = 1,2$)

1: **Initialize parameters:** $\theta_1^{(0)} = \hat{\theta}_1,\ \theta_2^{(0)} = \hat{\theta}_2$
2: Set iteration counter $j = 1$
3: **while** $j \leq \mathbb{C}$ **do**
4: Generate candidate values:
$\theta_1^{\star} \sim N(\hat{\theta}_1, \hat{\sigma}_{11}), \quad \theta_2^{\star} \sim N(\hat{\theta}_2, \hat{\sigma}_{22})$
5: Compute acceptance ratios:

$$\mho_{\theta_1} = \frac{P_{\theta_1}(\theta_1^{\star} \mid \bullet)}{P_{\theta_1}(\theta_1^{(j-1)} \mid \bullet)}, \quad \mho_{\theta_2} = \frac{P_{\theta_2}(\theta_2^{\star} \mid \bullet)}{P_{\theta_2}(\theta_2^{(j-1)} \mid \bullet)}$$

(Continued)

Algorithm 1 (continued)

6: Draw $u_1, u_2 \sim \text{Uniform}(0,1)$ and update samples:

$$\theta_1^{(j)} = \begin{cases} \theta_1^{\star}, & \text{if } u_1 \leq \min(1, \mho_{\theta_1}) \\ \theta_1^{(j-1)}, & \text{otherwise} \end{cases}, \quad \theta_2^{(j)} = \begin{cases} \theta_2^{\star}, & \text{if } u_2 \leq \min(1, \mho_{\theta_2}) \\ \theta_2^{(j-1)}, & \text{otherwise} \end{cases}$$

7: Increment iteration counter: $j = j + 1$

8: **end while**

9: Compute Bayes estimates of $\theta_i,\ i = 1, 2$ after burn-in $\mathbb{C}_0$ ($\mathbb{C}^{\star} = \mathbb{C} - \mathbb{C}_0$):

$$\tilde{\theta}_1 = \frac{1}{\mathbb{C}^{\star}} \sum_{j=\mathbb{C}_0+1}^{\mathbb{C}} \theta_1^{(j)}, \quad \tilde{\theta}_2 = \frac{1}{\mathbb{C}^{\star}} \sum_{j=\mathbb{C}_0+1}^{\mathbb{C}} \theta_2^{(j)}$$

10: Compute $(1-\mu)100\%$ BCI for $\theta_i,\ i = 1, 2$:

$$\left\{\theta_{1(0.5\mu\mathbb{C}^{\star})},\ \theta_{1((1-0.5\mu)\mathbb{C}^{\star})}\right\}, \quad \left\{\theta_{2(0.5\mu\mathbb{C}^{\star})},\ \theta_{2((1-0.5\mu)\mathbb{C}^{\star})}\right\}$$

11: Compute $(1-\mu)100\%$ HPD interval for $\theta_i,\ i = 1, 2$:

$$\left\{\theta_{1(j^{\star})},\ \theta_{1(j^{\star}+(1-\mu)\mathbb{C}^{\star})}\right\}, \quad \left\{\theta_{2(j^{\star})},\ \theta_{2(j^{\star}+(1-\mu)\mathbb{C}^{\star})}\right\}$$

where $j^{\star} = \mathbb{C}_0 + 1, \mathbb{C}_0 + 2, \ldots, \mathbb{C}$ is determined by

$$\theta_{1(j^{\star}+[(1-\mu)\mathbb{C}^{\star}])} - \theta_{1(j^{\star})} = \min_{1 \leqslant j \leqslant \mu\mathbb{C}^{\star}} \left[\theta_{1(j+[\mathbb{C}^{\star}(1-\mu)])} - \theta_{1(j)}\right].$$

12: Repeat Steps 10–11 for $\lambda_i,\ i = 1, 2$

5 Monte Carlo Comparisons

To evaluate the performance of the proposed estimators, exhaustive Monte Carlo simulations are performed using 5000 JT1-HC samples gathered by the sampling procedure described in Algorithm 2. These samples are drawn from two distinct configurations of NH $(\theta_i, \lambda_i),\ i = 1, 2$ populations:

- **Set A:** Population 1: NH(0.5, 1.5) and Population 2: NH(1.5, 0.5);
- **Set B:** Population 1: NH(1.0, 2.0) and Population 2: NH(2.0, 1.0).

Algorithm 2: The JT1-HC generation steps

1: **Input:** Set the number of replications N_{rep}

2: **Input:** Set the NH $(\theta_i, \lambda_i),\ i = 1, 2$, population parameters

3: **Input:** Set the censoring values for $n_i,\ i = 1, 2$, $t^{\star}$, and m

4: **Input:** For each replication $j = 1, \ldots, N_{rep}$, do

5: **Output:** Generate uniform random variates with n_1 as $v_x^{(j)} \sim \mathcal{U}(0,1)$ and with n_2 as $v_y^{(j)} \sim \mathcal{U}(0,1)$

6: **Output:** Compute $Q_x^{(j)} = G_x^{-1}(v_x^{(j)}; \theta_1, \lambda_1)$

7: **Output:** Compute $Q_y^{(j)} = G_y^{-1}(v_y^{(j)}; \theta_2, \lambda_2)$

8: **Output:** Compute $x^{(j)} = \text{sort}(Q_x^{(j)})$ and $y^{(j)} = \text{sort}(Q_y^{(j)})$

9: **Output:** Find d_j at $t^{\star}$ from $W^{(j)} = \{x^{(j)}, y^{(j)}\}$

(Continued)

Algorithm 2 (continued)

10: **Input:** Set FP100% = $\frac{m}{n^\star} \times 100\%$.

11: **Output:** Find indicators $\zeta_i^{(j)}$ for $i = 1, \ldots, m$

$$\zeta_i^{(j)} = \begin{cases} 1 & \text{if } \zeta_i^{(j)} \in x^{(j)}; \\ 0 & \text{otherwise.} \end{cases}$$

12: **Output:** Stop and collect

$$\mathcal{D}^\star = \begin{cases} m, & \text{if } m \le d_j; \\ d_j, & \text{if } m > d_j \end{cases}$$

$$W_{i,j}^{\text{new}} = \begin{cases} W_i^{(j)}, & \text{for } i = 1, 2, \ldots, \mathcal{D}_j^\star; \\ 0, & \text{for } i = \mathcal{D}_j^\star + 1, \ldots, n^\star \end{cases}$$

$$\mathcal{T}_j^\star = \begin{cases} W_{m,j}^{\text{new}}, & \text{if } m \le d_j; \\ t^\star, & \text{if } m > d_j \end{cases}$$

13: **Input:** Set $j = j + 1$ and redo Steps 5–13

To carry out this investigation, various values of the censoring time $t^\star$, sample sizes $n_i,\ i = 1, 2$, and the number of failures m are considered. Specifically, $t^\star$ was set to 1 and 2 for Set A, and to 0.2 and 0.5 for Set B. The sample sizes for both populations are chosen as $n_1(= 30,\ 50,\ 70)$ and $n_2(= 20,\ 50,\ 80)$.

The failure count m was determined as a percentage of the total number of items under test, with failure percentages (FP) defined as $\frac{m}{n^\star} \times 100\% = 30\%, 60\%$, and 90%. In this part, for the MLE optimization, we employed the NR algorithm was implemented via the `maxNR()` function in the `maxLik` package with a convergence tolerance of 10^{-6}. The initial parameter values were obtained using moment-based estimates from the observed uncensored sample or from exponential-model fits, which ensured rapid and stable convergence.

For the Bayesian analysis, we set the burn-in size to 2000 out of a total of 12,000 MCMC iterations. Furthermore, two sets of informative prior hyperparameters (a_{ij}, b_{ij}) for $i, j = 1, 2$ are adopted based on the criteria introduced by Kundu [25]. The values of the hyperparameters a_{ij} and b_{ij} (for $i, j = 1, 2$) in this part are chosen to reflect moderate prior information consistent with the parameter magnitudes observed in actual NH distribution parameters. Specifically, we assign two sets of priors called "Prior 1" and "Prior 2", which correspond to weakly informative and moderately informative cases, respectively.

The considered priors are specified as follows:

- **Set A:**
  - Prior 1: $(a_{ii}, b_{ii}) = (2.5, 5),\ i = 1, 2$, and $(a_{ij}, b_{ij}) = (7.5, 5),\ i, j = 1, 2$;
  - Prior 2: $(a_{ii}, b_{ii}) = (5, 10),\ i = 1, 2$, and $(a_{ij}, b_{ij}) = (15, 10),\ i, j = 1, 2$,
- **Set B:**
  - Prior 1: $(a_{ii}, b_{ii}) = (5, 5),\ i = 1, 2$, and $(a_{ij}, b_{ij}) = (10, 5),\ i, j = 1, 2$;
  - Prior 2: $(a_{ii}, b_{ii}) = (10, 10),\ i = 1, 2$, and $(a_{ij}, b_{ij}) = (20, 10),\ i, j = 1, 2$.

For $j \in \{1, 2, \ldots, N_{rep}\}$, the average point estimate (APEs), as provided in Eq. (24), of the parameters θ_i and λ_i (for $i = 1, 2$), say Υ for short, is computed as follows:

$$\mathrm{APE}(\ddot{\Upsilon}) = \frac{1}{N_{rep}} \sum_{j=1}^{N_{rep}} \ddot{\Upsilon}^{(j)}, \tag{24}$$

where $\ddot{\Upsilon}^{(j)}$ denotes the estimated value of Υ from the jth replication.

To further assess the accuracy of the estimates, we evaluate their root mean squared errors (RMSEs) and mean absolute biases (MABs), provided by Eqs. (25) and (26):

$$\mathrm{RMSE}(\ddot{\Upsilon}) = \sqrt{\frac{1}{N_{rep}} \sum_{j=1}^{N_{rep}} \left(\ddot{\Upsilon}^{(j)} - \Upsilon\right)^2}, \tag{25}$$

$$\mathrm{MAB}(\ddot{\Upsilon}) = \frac{1}{N_{rep}} \sum_{j=1}^{N_{rep}} \left|\ddot{\Upsilon}^{(j)} - \Upsilon\right|, \tag{26}$$

respectively.

Additionally, the precision of the 95% asymptotic and credible intervals for Υ is evaluated using the average interval length (AIL) and coverage probability (CP), provided by Eqs. (27) and (28):

$$\mathrm{AIL}_{95\%}(\Upsilon) = \frac{1}{N_{rep}} \sum_{j=1}^{N_{rep}} \left(\mathsf{U}_{\ddot{\Upsilon}^{(j)}} - \mathsf{L}_{\ddot{\Upsilon}^{(j)}}\right), \tag{27}$$

$$\mathrm{CP}_{95\%}(\Upsilon) = \frac{1}{N_{rep}} \sum_{j=1}^{N_{rep}} \zeta^{\star}\left(\mathsf{L}_{\ddot{\Upsilon}^{(j)}}; \mathsf{U}_{\ddot{\Upsilon}^{(j)}}\right)(\Upsilon), \tag{28}$$

where $\zeta^{\star}(\cdot)$ is the indicator function, and $(\mathsf{L}(\cdot), \mathsf{U}(\cdot))$ denote the (lower,upper) bounds of the asymptotic (or credible) intervals.

All calculations were performed using R x64 4.2.2 on Windows 10 using an HP laptop with a Core(TM) i5-5200U processor and 8.00 GB of RAM. To distinguish, in Tables A1–A4, the point estimation results of θ_i and λ_i (for $i = 1, 2$) are listed, respectively, while the interval estimation results of θ_i and λ_i (for $i = 1, 2$) are listed in Tables A5–A8, respectively. For short, the point and interval simulated results of θ_i and λ_i (for $i = 1, 2$) are moved to Appendix B. In terms of the lowest RMSE, MAB, and AIL values as well as the highest CP values, we state the following comments:

- The estimation results for both θ_i and λ_i ($i = 1, 2$) demonstrate overall effectiveness across all considered scenarios.
- As the sample sizes n_i, $i = 1, 2$, grow, the precision of all estimators for θ_i and λ_i ($i = 1, 2$) improves accordingly. A similar trend is observed when the level of FP% increases.
- With increasing values of $t^{\star}$, for both sets A and B, the RMSE, MABs, and AILs associated with the estimates of θ_i and λ_i (for $i = 1, 2$) tend to decrease, while the corresponding values of CPs increase.
- As the true parameter values of θ_i and λ_i ($i = 1, 2$) increase, we noticed that the RMSE, MAB, and AIL results for all estimators of θ_i or λ_i (for $i = 1, 2$) increased while their CP results decreased.
- The Bayesian estimates for θ_i and λ_i ($i = 1, 2$), utilizing informative gamma priors, generally outperform the competitive frequentist approach. Similar superiority is observed in the associated BCI/HPD interval estimations.

- Across all simulation setups, the Bayesian MCMC results under Prior 2 consistently yield more efficient estimates compared to Prior 1. This improvement is attributed to the lower variance associated with Prior 2, which enhances estimation stability.
- A comparison of interval estimation results reveals the following:
  - From the asymptotic setups, the ACI-NL method yields more accurate interval estimates for $\theta_i,\ i = 1, 2$, whereas the ACI-NA method performs better in estimating $\lambda_i,\ i = 1, 2$.
  - Among the credible interval approaches, the HPD method yields the most precise estimates for θ_i and λ_i $(i = 1, 2)$ compared to the BCI method, while both Bayesian methods outperform those obtained using the ACI-NL and ACI-NA approaches.

  To sum up, when a JT1-HC sample is available, the Bayesian Metropolis–Hastings framework is recommended for estimating the parameters of two independent Nadarajah-Haghighi lifespan populations, owing to its superior accuracy and interval performance.

6 Jointly Data Applications

To demonstrate the applicability of the proposed methods to real-world scenarios, this section analyzes three real datasets: (1) the first involving the evaluation of two technologies used to determine unit capacity characteristics; (2) the second measuring the time between mechanical equipment failures that are repairable; and (3) the third comprising the failure times of air-conditioning systems in Boeing aircraft. In Table 1, the two groups of failure times are denoted by $\mathbb{X}$ and $\mathbb{Y}$, and the datasets are detailed as follows:

- **Data [1]:** Capacity factor failures for two algorithms, namely "SC16" and "P3"; see Bayoud and Raqab [26], and Alqasem et al. [27].
- **Data [2]:** Time between failures (in hours) for 30 mechanical equipment items. Originally reported by Murthy et al. [28] and later reanalyzed by Elshahhat et al. [9].
- **Data [3]:** Time intervals (in hours) between consecutive failures of the air-conditioning systems in a fleet of 13 Boeing 720 jet airplanes "7913" and "7914". The data was first introduced by Proschan [29] and subsequently examined by Abo-Kasem and Elshahhat [30].

Briefly, the flexibility and superiority of the proposed NH distribution are demonstrated by comparing its fit to the complete datasets reported in Table 1 against five competing two- and three-parameter lifetime models, namely the power generalized Weibull (PGW $(\alpha, \theta, \lambda)$) by Bagdonavicius and Nikulin [31]; new extended Weibull (NEW $(\alpha, \theta, \lambda)$) by Peng and Yan [32]; Harris-extended-exponential (HEE $(\alpha, \theta, \lambda)$) by Pinho et al. [33]; alpha-power-exponential (APE (θ, λ)) by Mahdavi and Kundu [34]; Birnbaum–Saunders (BS (θ, λ)) by Birnbaum and Saunders [35] models.

Table 1: Groups of failure times in the three engineering datasets.

Data	(n_1, n_2)	Group	Times									
Data [1]	(23, 22)	$\mathbb{X}$	0.06	0.08	0.11	0.14	0.21	0.29	0.36	0.48	0.59	0.70
			0.92	1.16	1.16	2.13	3.44	4.03	4.92	5.44	7.17	7.59
			8.09	8.53	8.66							
		$\mathbb{Y}$	0.10	0.14	0.19	0.26	0.36	0.44	0.56	0.67	0.78	0.97
			1.18	1.18	2.07	3.34	3.99	5.03	5.57	7.16	7.59	8.00
			8.53	8.74								

(Continued)

Table 1 (continued)

Data	(n_1, n_2)	Group	Times									
Data [2]	(15, 15)	$\mathbb{X}$	0.11	0.45	0.63	0.70	0.71	0.77	1.17	1.23	1.24	1.43
			1.74	1.86	1.97	2.23	4.36					
		$\mathbb{Y}$	0.30	0.40	0.59	0.74	0.94	1.06	1.23	1.46	1.49	1.82
			2.37	2.46	2.63	3.46	4.73					
Data [3]	(27, 24)	$\mathbb{X}$	1	4	11	16	18	18	18	24	31	39
			46	51	54	63	68	77	80	82	97	106
			111	141	142	163	191	206	216			
		$\mathbb{Y}$	3	5	5	13	14	15	22	22	23	30
			36	39	44	46	50	72	79	88	97	102
			139	188	197	210						

To identify the best-fitting model, several model selection criteria are employed, including the Akaike information (AI), consistent Akaike information (CAI), Bayesian information (BI), Hannan–Quinn information (HQI), and the Kolmogorov–Smirnov (KS) test statistic along with its associated p-value. All fitting metrics are computed using the AdequacyModel package developed by Marinho et al. [36]. To this end, the MLE of each model parameter (along with the corresponding standard error (Std.E)) and the corresponding results for the fit criteria are obtained and summarized in Table 2. It reveals that the proposed NH lifespan model fits the three datasets proposed satisfactorily. Additionally, it indicates that the NH distribution produces the lowest values across all considered model selection criteria, while achieving the highest associated p-value for all groups in the three datasets. In contrast, based on KS (p-value), for Data [2] (set $\mathbb{X}$), the PGW, NEW, HEE, and APE models outperform the NH model. This outcome clearly demonstrates that the NH model offers a superior fit to the data compared to the competing lifetime models. To visually support this conclusion, Figs. 2 and 3 show the fitted/empirical CDF lines, fitted/empirical quantile–quantile (QQ) lines, log-likelihood contour, and boxplot-within-violin, based on the grouped data $\mathbb{X}$ and $\mathbb{Y}$ in Table 1. As expected, subplots (a)–(b) in Figs. 2 and 3 further confirm the satisfactory fit of the NH model, consistent with the results presented in Table 2. Subplot (c) in Figs. 2 and 3 also demonstrates that the fitted estimates of $\hat{\theta}i$ and $\hat{\lambda}i$ for $i = 1, 2$ exist and are unique. We recommend using the corresponding values of $\hat{\theta}i$ and $\hat{\lambda}i$ for $i = 1, 2$ as initial guesses in subsequent computations.

Table 2: Fitting summary of the NH model and its competitors from three engineering datasets.

Data	Group	Model	α		θ		λ		AI	CAI	BI	HQI	KS	p-value
			Est.	Std.E	Est.	Std.E	Est.	Std.E						
Data [1]	$\mathbb{X}$	NH	–	–	0.4367	0.1510	1.8866	1.6166	95.711	96.311	97.982	96.282	0.1470	0.7029
		PGW	0.0473	0.1508	0.5987	0.1241	8.2930	25.477	96.502	97.765	99.908	97.358	0.1604	0.5945
		NEW	0.0838	0.0662	0.6125	0.1453	0.6535	0.2005	95.744	96.407	98.150	96.304	0.1493	0.7023
		HEE	0.0131	0.0937	3.5009	23.351	8.9284	59.056	100.44	101.71	103.85	101.30	0.2065	0.2805
		APE	–	–	0.2430	0.3258	0.2533	0.1109	97.078	97.678	99.349	97.649	0.1656	0.5533
		BS	–	–	1.9446	0.2876	0.9561	0.2557	95.818	96.428	98.035	96.453	0.1507	0.6733
	$\mathbb{Y}$	NH	–	–	0.5694	0.2475	0.9415	0.8728	95.882	96.514	98.064	96.396	0.1362	0.8093
		PGW	0.0415	0.1199	0.6679	0.1395	8.1443	22.726	97.150	98.484	100.42	97.921	0.1851	0.4378
		NEW	0.1491	0.1226	0.6706	0.1739	0.5830	0.2103	95.951	96.840	98.780	96.778	0.1365	0.8068

(Continued)

Table 2 (continued)

Data	Group	Model	α		θ		λ		AI	CAI	BI	HQI	KS	*p*-value
			Est.	Std.E	Est.	Std.E	Est.	Std.E						
		HEE	0.0120	0.2014	1.1125	15.246	3.2841	44.535	98.888	100.22	102.16	99.659	0.2174	0.2494
		APE	–	–	0.3345	0.4604	0.2556	0.1129	96.062	96.694	98.244	96.576	0.1727	0.5280
		BS	–	–	1.6578	0.2507	1.2497	0.3199	96.046	96.636	98.787	97.119	0.1405	0.7777
Data [2]	𝕏	NH	–	–	3.2776	4.7897	0.1558	0.2732	41.776	42.776	43.192	41.761	0.1684	0.7284
		PGW	1.1297	1.4956	1.8098	0.7702	0.5856	0.4913	42.089	44.270	44.213	42.066	0.1086	0.9860
		NEW	0.0667	0.2248	1.3928	0.3602	0.5928	0.2602	42.281	44.463	44.405	42.258	0.1110	0.9825
		HEE	3.1580	4.1784	1.1288	0.4527	7.7638	10.257	41.873	43.910	43.852	41.791	0.1157	0.9740
		APE	–	–	19.746	28.740	1.3107	0.3306	41.862	42.862	43.239	41.778	0.1000	0.9945
		BS	–	–	0.9341	0.1708	0.9454	0.2051	43.418	44.418	44.834	43.403	0.1975	0.5375
	𝕐	NH	–	–	8.5129	29.207	0.0438	0.1612	47.825	48.825	49.241	47.810	0.1109	0.9827
		PGW	0.9318	1.6800	1.9419	1.0882	0.5066	0.5898	48.416	50.598	50.540	48.393	0.1147	0.9811
		NEW	0.4805	0.6053	1.1460	0.5101	0.6626	0.5048	47.870	50.052	49.994	47.847	0.1197	0.9817
		HEE	20.882	20.618	0.6937	0.1904	54.361	139.22	48.301	50.483	50.425	48.278	0.1128	0.9822
		APE	–	–	17.168	26.437	1.0257	0.2767	47.918	48.892	49.340	47.884	0.1183	0.9805
		BS	–	–	0.8028	0.1466	1.2920	0.2467	47.861	48.922	49.373	47.841	0.1119	0.9811
Data [3]	𝕏	NH	–	–	1.7515	0.8219	0.0059	0.0037	291.23	291.73	293.82	292.00	0.0812	0.9921
		PGW	0.0079	0.0053	1.0678	0.2248	1.1303	0.7741	293.73	294.78	297.62	294.89	0.0841	0.9912
		NEW	0.2136	1.2687	1.0943	0.1500	0.0084	0.0061	293.91	294.95	297.79	295.06	0.0868	0.9905
		HEE	0.0303	0.0991	0.1541	0.4610	15.958	48.371	292.88	293.92	296.76	294.03	0.0939	0.9712
		APE	–	–	2.5875	2.8519	0.0162	0.0044	291.80	292.30	294.39	292.57	0.0885	0.9841
		BS	–	–	1.6236	0.2245	29.653	6.9657	304.05	304.55	306.64	304.82	0.2386	0.0924
	𝕐	NH	–	–	1.0188	0.5211	0.0152	0.0126	251.72	252.13	254.07	252.12	0.0850	0.9951
		PGW	0.0151	0.0117	1.1301	0.4836	0.7225	0.8213	253.64	254.84	257.18	254.58	0.0871	0.9928
		NEW	3.7060	4.1758	0.8976	0.1993	0.0264	0.0255	252.68	253.88	256.21	253.61	0.0902	0.9900
		HEE	0.0639	0.4877	0.0270	0.0870	1.8130	5.9791	253.68	254.88	257.21	254.61	0.0930	0.9855
		APE	–	–	0.8860	1.2047	0.0152	0.0060	251.93	252.38	254.17	252.35	0.0888	0.9928
		BS	–	–	1.3225	0.1910	33.2703	7.2517	251.96	252.75	254.32	252.58	0.1264	0.8380

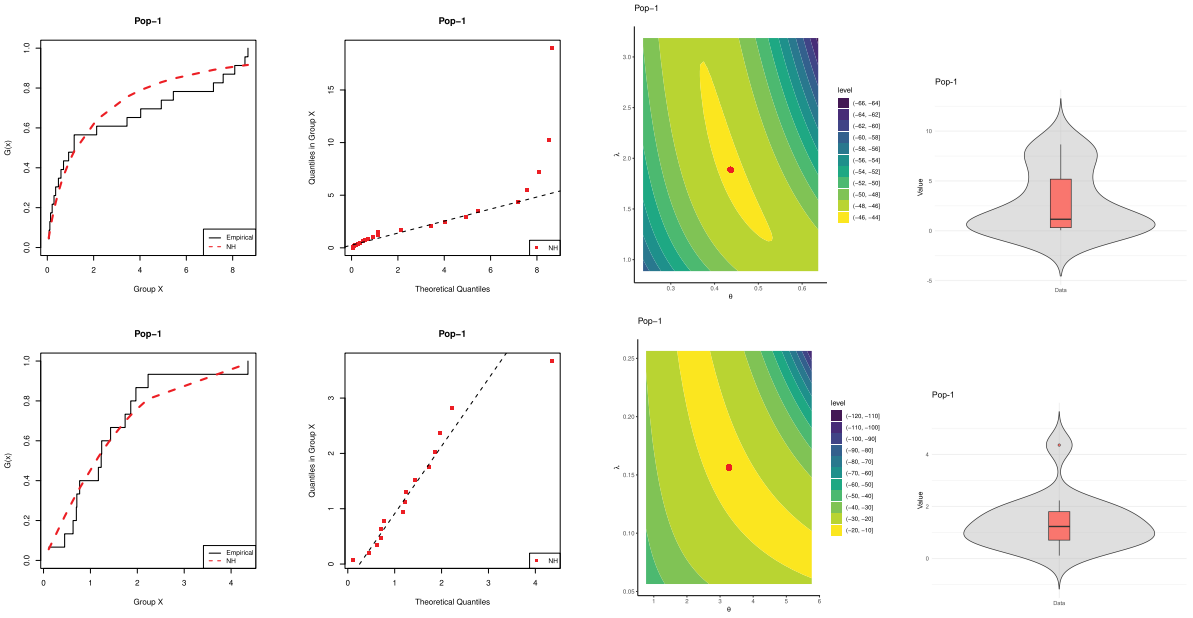
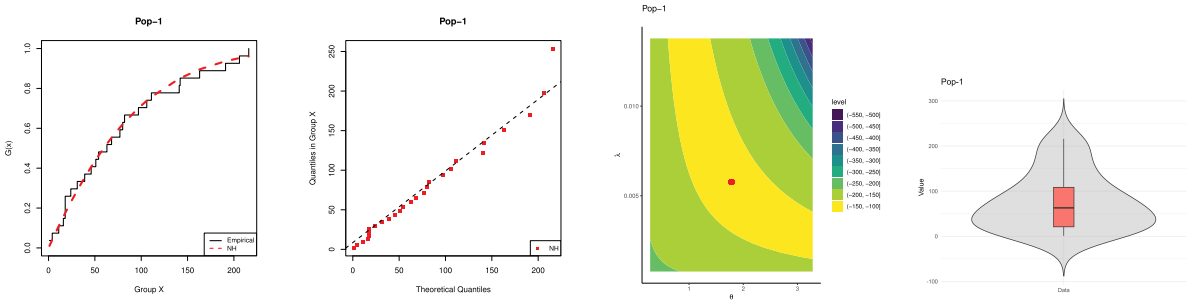
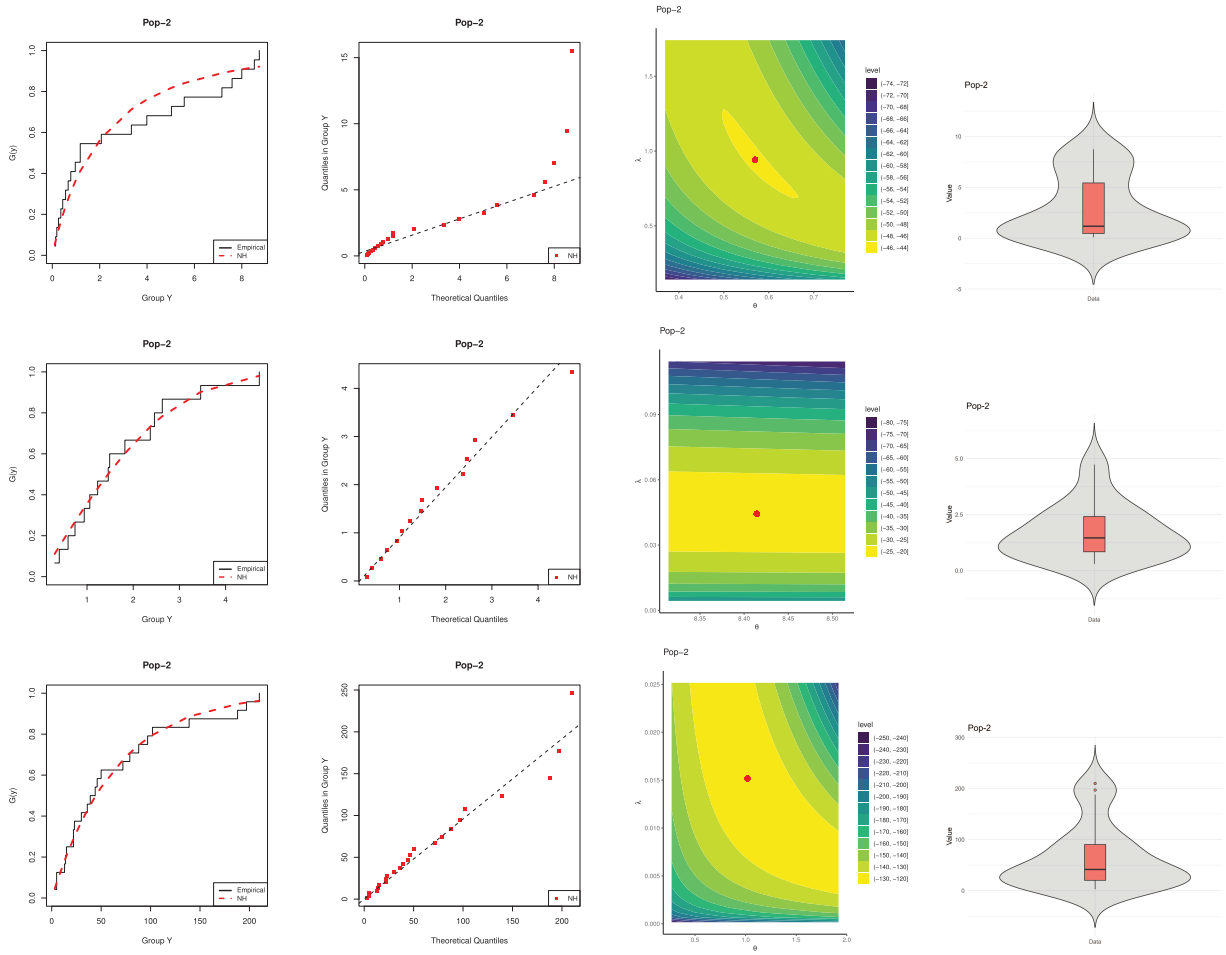


Figure 2: (Continued)



(a) CDF (b) QQ (c) Contour (d) Violin

Figure 2: Fitting diagrams of the NH model using group-$\mathbb{X}$ in the three engineering datasets.



(a) CDF (b) QQ (c) Contour (d) Violin

Figure 3: Fitting diagrams of the NH model using group-$\mathbb{Y}$ in the three engineering datasets.

From Table 1, various JT1-HC samples are generated based on different choices of τ, with $m = 20, 15$, and 25 for Data $[i]$ (where $i = 1, 2, 3$), respectively; see Table 3. For each case $\mathbb{S}[ij]$, where $i, j = 1, 2, 3$, the maximum likelihood and Bayesian estimates (along with their Std.Es), as well as the asymptotic and credible interval estimates (with their interval widths (IWs)), are computed for the parameters θ_i and λ_i for $i =$

1, 2; see Table 4. Since no prior information is available for the hyperparameters (a_{ij}, b_{ij}) for $i, j = 1, 2$, the Bayesian point and 95% HPD interval estimates are obtained under non-informative gamma priors. The numerical results in Table 4 show that the Bayesian estimates of θ_i and λ_i (for $i = 1, 2$) generally outperform the frequentist estimates in terms of smaller Std.E values. Furthermore, both the 95% BCI and HPD interval estimates yield narrower IW values than the corresponding 95% ACI-NA and ACI-NL results, indicating greater precision.

Table 3: Various JT1-HC samples from the three engineering datasets.

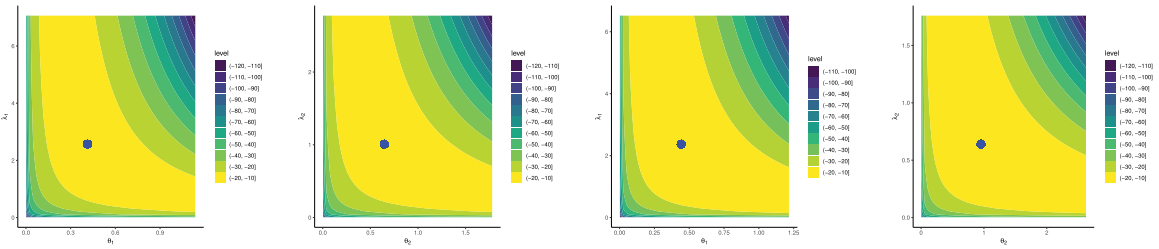
Data	Sample	$t^\star(d)$	$w_i[\zeta_i]$					$n_1^\star$	$n_2^\star$	$\mathcal{T}^\star$	$\mathcal{D}_j^\star$
Data [1]	$\mathbb{S}[11]$	0.95(20)	0.06 [1]	0.08 [1]	0.10 [2]	0.11 [1]	0.14 [2]	12	13	0.92	20
			0.14 [1]	0.19 [2]	0.21 [1]	0.26 [2]	0.29 [1]				
			0.36 [1]	0.36 [2]	0.44 [2]	0.48 [1]	0.56 [2]				
			0.59 [1]	0.67 [2]	0.70 [1]	0.78 [2]	0.92 [1]				
	$\mathbb{S}[12]$	0.75(18)	0.06 [1]	0.08 [1]	0.10 [2]	0.11 [1]	0.14 [2]	13	14	0.75	18
			0.14 [1]	0.19 [2]	0.21 [1]	0.26 [2]	0.29 [1]				
			0.36 [1]	0.36 [2]	0.44 [2]	0.48 [1]	0.56 [2]				
			0.59 [1]	0.67 [2]	0.70 [1]						
Data [2]	$\mathbb{S}[21]$	1.25(15)	0.11 [1]	0.30 [2]	0.40 [2]	0.45 [1]	0.59 [2]	7	8	1.23	15
			0.63 [1]	0.70 [1]	0.71 [1]	0.74 [2]	0.77 [1]				
			0.94 [2]	1.06 [2]	1.17 [1]	1.23 [2]	1.23 [1]				
	$\mathbb{S}[22]$	1.10(12)	0.11 [1]	0.30 [2]	0.40 [2]	0.45 [1]	0.59 [2]	9	9	1.10	12
			0.63 [1]	0.70 [1]	0.71 [1]	0.74 [2]	0.77 [1]				
			0.94 [2]	1.06 [2]							
Data [3]	$\mathbb{S}[31]$	50(25)	1 [1]	3 [2]	4 [1]	5 [2]	5 [2]	13	13	50	25
			11 [1]	13 [2]	14 [2]	15 [2]	16 [1]				
			18 [1]	18 [1]	18 [1]	22 [2]	22 [2]				
			23 [2]	24 [1]	30 [2]	31 [1]	36 [2]				
			39 [2]	39 [1]	44 [2]	46 [2]	46 [1]				
	$\mathbb{S}[32]$	40(20)	1 [1]	3 [2]	4 [1]	5 [2]	5 [2]	15	16	40	20
			11 [1]	13 [2]	14 [2]	15 [2]	16 [1]				
			18 [1]	18 [1]	18 [1]	22 [2]	22 [2]				
			23 [2]	24 [1]	30 [2]	31 [1]	36 [2]				

Using $\mathbb{S}[ii]$ from Data $[i]$ for $i = 1, 2, 3$, Fig. 4 presents the log-likelihood contour plots for θ_i and λ_i $(i = 1, 2, 3)$. All subplots in Fig. 4 confirm the existence and uniqueness of the MLEs $\hat{\theta}i$ and $\hat{\lambda}i$ $(i = 1, 2, 3)$, consistent with the fitted values reported in Table 4. Additionally, Fig. 5 displays the posterior density and trace plots of θ_i and λ_i $(i = 1, 2, 3)$, based on the same $\mathbb{S}[ii]$ samples from Data [1] as representative cases. These plots demonstrate satisfactory convergence of the MCMC chains and confirm that the chosen burn-in size of 10,000 iterations is sufficient to eliminate the influence of the initial values. The distribution of the 40,000 retained samples indicates that the posterior distribution of θ_i (or λ_i) for $i = 1, 2, 3$ is approximately symmetric. A range of descriptive statistics, including posterior mean, mode, quartiles $(\mathbb{Q}_i,\ i = 1, 2, 3)$, standard deviation (Std.D), and skewness (Skew.), are calculated based on 40,000 posterior samples of the

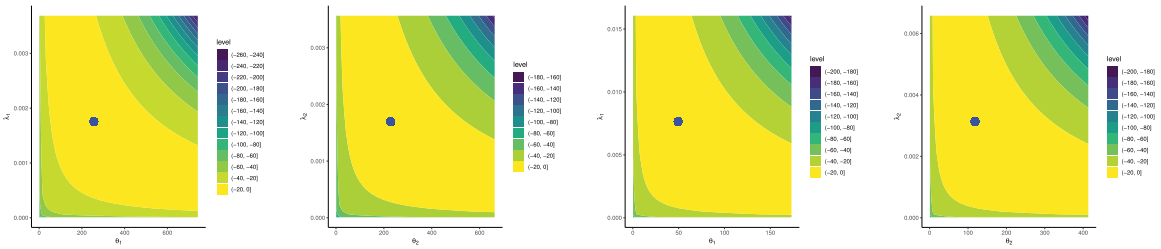
parameters θ_i and λ_i (for $i = 1, 2$), as presented in Table 5. These summaries align with the estimation results listed in Table 4 and further support the patterns shown in Fig. 5.

Table 4: Estimates of θ_i and λ_i (for $i = 1, 2$) from the three engineering datasets.

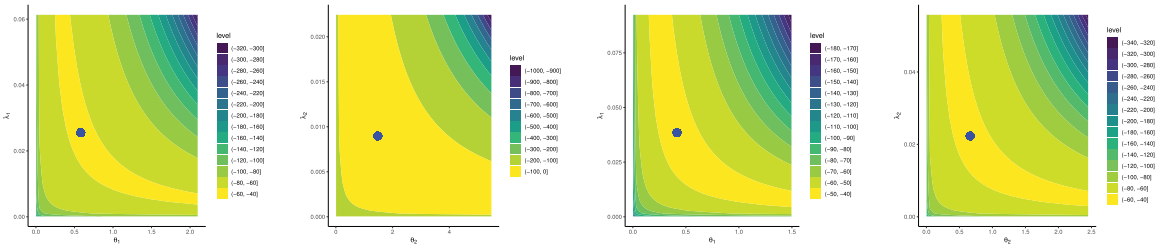
Data	Sample	Par.	MLE		Bayes		95% ACI-NA 95% ACI-NL			95% BCI 95% HPD		
			Est.	Std.E	Est.	Std.E	Low.	Upp.	IW	Low.	Upp.	IW
Data [1]	$\mathbb{S}[11]$	θ_1	0.4133	0.3502	0.3893	0.0508	0.0000	1.0996	1.0996	0.3028	0.4773	0.1745
							0.0785	2.1753	2.0968	0.3028	0.4773	0.1745
		θ_2	0.6467	1.0404	0.6209	0.0548	0.0000	2.6858	2.6858	0.5265	0.7151	0.1886
							0.0276	15.138	15.110	0.5265	0.7151	0.1886
		λ_1	2.5674	3.5371	2.5421	0.0567	0.0000	9.5000	9.5000	2.4436	2.6397	0.1960
							0.1725	38.210	67.462	2.4436	2.6397	0.1960
		λ_2	1.0090	2.1636	0.9837	0.0556	0.0000	5.2496	5.2496	0.8862	1.0805	0.1943
							0.0151	67.477	38.038	0.8862	1.0805	0.1943
	$\mathbb{S}[12]$	θ_1	0.4422	0.4738	0.4180	0.0518	0.0000	1.3710	1.3710	0.3287	0.5090	0.1803
							0.0542	3.6116	3.5574	0.3287	0.5090	0.1803
		θ_2	0.9541	2.6523	0.9287	0.0551	0.0000	6.1526	6.1526	0.8329	1.0251	0.1923
							0.0041	221.77	221.76	0.8329	1.0251	0.1923
		λ_1	2.3709	3.8908	2.3464	0.0547	0.0000	9.9968	9.9968	2.2539	2.4433	0.1893
							0.0951	59.133	436.43	2.2539	2.4433	0.1893
		λ_2	0.6398	2.1302	0.6137	0.0551	0.0000	4.8149	4.8149	0.5200	0.7093	0.1893
							0.0009	436.43	59.037	0.5200	0.7093	0.1893
Data [2]	$\mathbb{S}[21]$	θ_1	255.99	14.042	255.99	0.0020	228.47	283.51	55.043	255.99	255.99	0.0008
							229.90	285.05	55.149	255.99	255.99	0.0008
		θ_2	228.51	14.049	228.51	0.0020	200.97	256.04	55.070	228.51	228.51	0.0008
							202.57	257.77	55.204	228.51	228.51	0.0008
		λ_1	0.0018	0.0005	0.0017	0.0018	0.0008	0.0027	0.0019	0.0014	0.0021	0.0007
							0.0010	0.0030	0.0022	0.0014	0.0021	0.0007
		λ_2	0.0017	0.0005	0.0017	0.0019	0.0007	0.0027	0.0021	0.0013	0.0020	0.0007
							0.0009	0.0031	0.0020	0.0013	0.0020	0.0007
	$\mathbb{S}[22]$	θ_1	49.452	3.6223	49.452	0.0020	42.352	56.552	14.199	49.452	49.452	0.0008
							42.838	57.086	14.248	49.452	49.452	0.0008
		θ_2	118.10	8.6102	118.10	0.0020	101.23	134.98	33.751	118.10	118.10	0.0008
							102.38	136.24	33.866	118.10	118.10	0.0008
		λ_1	0.0076	0.0027	0.0076	0.0020	0.0024	0.0129	0.0104	0.0073	0.0080	0.0008
							0.0039	0.0151	0.0046	0.0073	0.0080	0.0008
		λ_2	0.0031	0.0011	0.0031	0.0020	0.0010	0.0053	0.0042	0.0027	0.0035	0.0008
							0.0016	0.0062	0.0112	0.0027	0.0035	0.0008
Data [3]	$\mathbb{S}[31]$	θ_1	0.5830	0.7233	0.5830	0.0100	0.0000	2.0007	2.0007	0.5810	0.5849	0.0039
							0.0512	6.6337	6.5825	0.5810	0.5849	0.0039
		θ_2	1.4815	3.8467	1.4815	0.0100	0.0000	9.0209	9.0209	1.4796	1.4835	0.0039
							0.0091	240.32	240.31	1.4796	1.4835	0.0039
		λ_1	0.0255	0.0450	0.0255	0.0099	0.0000	0.1137	0.1137	0.0236	0.0275	0.0039
							0.0008	0.8058	3.7051	0.0236	0.0275	0.0039
		λ_2	0.0090	0.0276	0.0089	0.0092	0.0000	0.0630	0.0630	0.0071	0.0107	0.0036
							0.0000	3.7051	0.8050	0.0071	0.0107	0.0036
	$\mathbb{S}[32]$	θ_1	0.4155	0.4874	0.4155	0.0100	0.0000	1.3708	1.3708	0.4135	0.4175	0.0039
							0.0417	4.1401	4.0984	0.4135	0.4175	0.0039
		θ_2	0.6621	1.0145	0.6621	0.0100	0.0000	2.6505	2.6505	0.6602	0.6641	0.0039
							0.0329	13.339	13.306	0.6602	0.6641	0.0039
		λ_1	0.0385	0.0667	0.0385	0.0099	0.0000	0.1691	0.1691	0.0365	0.0404	0.0039
							0.0013	1.1461	1.1868	0.0365	0.0404	0.0039
		λ_2	0.0223	0.0452	0.0223	0.0099	0.0000	0.1110	0.1110	0.0203	0.0242	0.0039
							0.0004	1.1872	1.1449	0.0203	0.0242	0.0039



(a) Data[1]

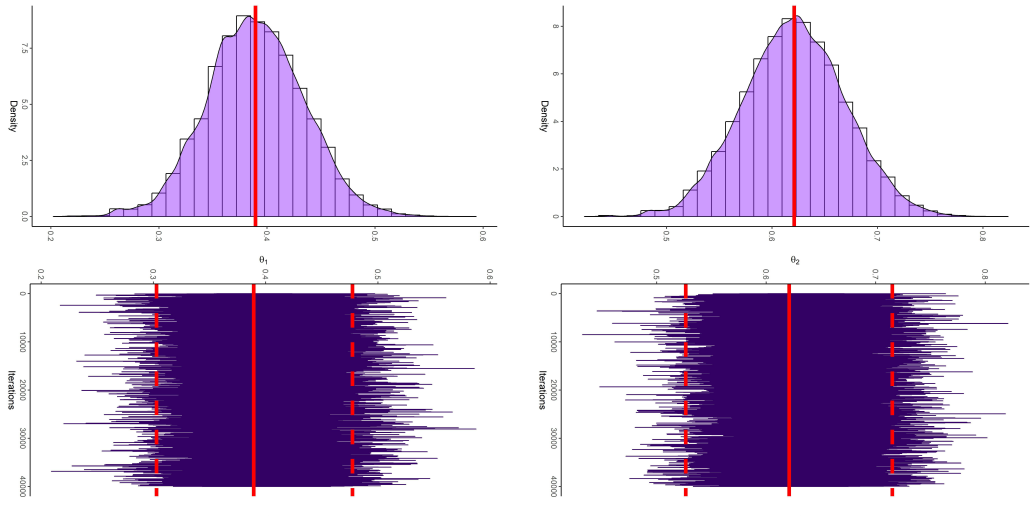


(b) Data[2]



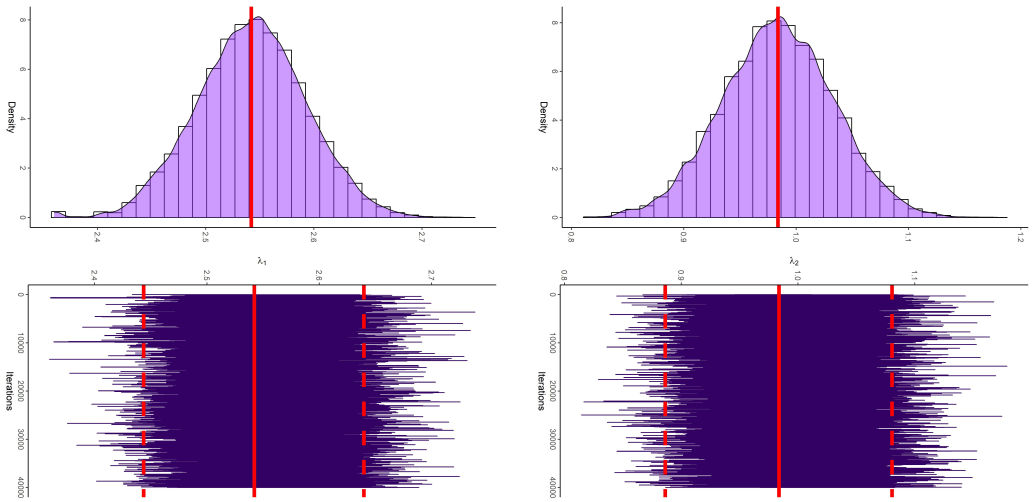
(c) Data[3]

Figure 4: The log-likelihood contours of θ_i and λ_i (for $i = 1, 2$) from the three engineering datasets.



(a) θ_1 (b) θ_2

Figure 5: (Continued)



(c) λ_1 (d) λ_2

Figure 5: The density and trace diagrams of θ_i and λ_i (for $i = 1, 2$) from data [1].

Table 5: Statistics summary for 40,000 MCMC iterations of θ_i and λ_i (for $i = 1, 2$) from the three engineering datasets.

Data	Sample	Par.	Mean	$\mathbb{Q}_1$	$\mathbb{Q}_2$	$\mathbb{Q}_3$	Mode	Std.D	Skew.
Data [1]	$\mathbb{S}[11]$	θ_1	0.38932	0.36000	0.35929	0.38878	0.41923	0.04482	0.01097
		θ_2	0.62095	0.54247	0.58848	0.62123	0.65363	0.04834	−0.01287
		λ_1	2.54214	2.36083	2.50835	2.54289	2.57606	0.05071	−0.08967
		λ_2	0.98374	1.01368	0.95024	0.98396	1.01695	0.04950	−0.01471
	$\mathbb{S}[12]$	θ_1	0.41800	0.38486	0.38730	0.41795	0.44848	0.04573	0.01740
		θ_2	0.92868	0.82483	0.89569	0.92882	0.96224	0.04887	0.01394
		λ_1	2.34637	2.32853	2.31334	2.34573	2.37900	0.04890	0.05771
		λ_2	0.61372	0.55531	0.58042	0.61363	0.64648	0.04846	0.04769
Data [2]	$\mathbb{S}[21]$	θ_1	255.990	255.990	255.990	255.990	255.990	0.00200	−0.01928
		θ_2	228.508	228.508	228.508	228.508	228.508	0.00199	0.02562
		λ_1	0.00174	0.00154	0.00162	0.00174	0.00187	0.00184	0.03552
		λ_2	0.00168	0.00138	0.00155	0.00168	0.00181	0.00186	0.01773
	$\mathbb{S}[22]$	θ_1	49.4520	49.4521	49.4518	49.4520	49.4521	0.00200	−0.01122
		θ_2	118.104	118.104	118.103	118.104	118.104	0.00199	0.01669
		λ_1	0.00765	0.00746	0.00751	0.00764	0.00778	0.00198	0.03011
		λ_2	0.00312	0.00287	0.00299	0.00312	0.00325	0.00196	−0.00199
Data [3]	$\mathbb{S}[31]$	θ_1	0.58298	0.58250	0.58230	0.58298	0.58366	0.01002	−0.02051
		θ_2	1.48153	1.48094	1.48085	1.48153	1.48220	0.00995	0.02023
		λ_1	0.02551	0.02419	0.02485	0.02551	0.02618	0.00988	0.02293
		λ_2	0.00890	0.00875	0.00827	0.00889	0.00951	0.00913	0.04135
	$\mathbb{S}[32]$	θ_1	0.41552	0.41635	0.41484	0.41551	0.41619	0.01001	−0.01250
		θ_2	0.66211	0.66161	0.66143	0.66211	0.66278	0.00996	0.01888
		λ_1	0.03847	0.03757	0.03780	0.03847	0.03914	0.00994	0.03196

(Continued)

Table 5 (continued)

Data	Sample	Par.	Mean	$\mathbb{Q}_1$	$\mathbb{Q}_2$	$\mathbb{Q}_3$	Mode	Std.D	Skew.
		λ_2	0.02226	0.02098	0.02160	0.02226	0.02293	0.00987	0.00008

In reliability analysis, estimating the mean lifetime (EML) of the proposed NH population is of particular importance. To this end, using the MLEs $\hat{\theta}_i$ and $\hat{\lambda}_i$ for $i = 1, 2$ (as reported in Table 4), the EMLs of the NH lifetime distributions for groups $\mathbb{X}$ and $\mathbb{Y}$ are computed and illustrated in Fig. 6. The observed patterns in EMLs highlight notable differences in reliability behavior between the two groups across the datasets. Specifically, the consistently higher EMLs for group **X** in Data-$[i]$ for $i = 1, 3$, suggest superior longevity or performance characteristics compared to group **Y**. However, the opposite of this trend in Data [2], meaning implies that group-level reliability is context-dependent and may vary under different operational or environmental conditions. Therefore, it is recommended that decision-makers consider group-level EML trends alongside covariate effects to improve reliability-based classification.

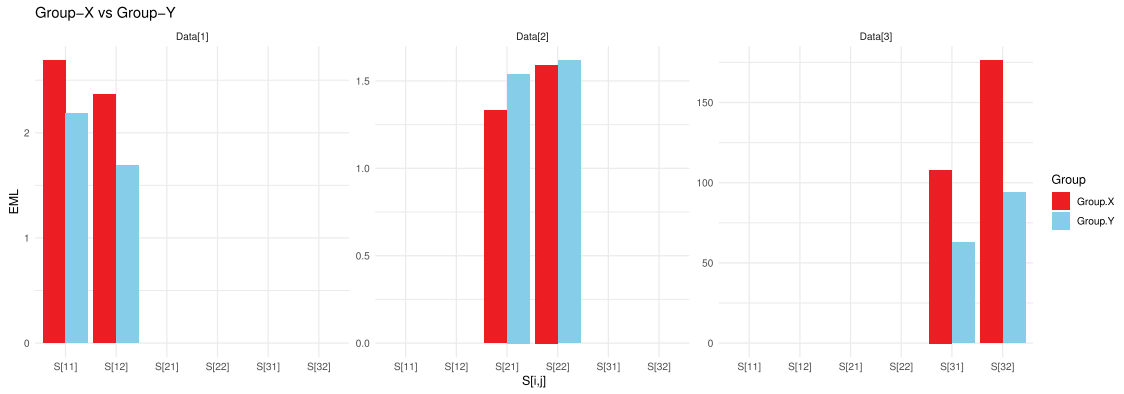


Figure 6: The EMLs of the NH populations from the three engineering datasets.

Ultimately, the engineering analyses demonstrate that the proposed methods yield strong performance on real-world data and offer clear insights into the behavior of the NH lifespan model when samples are obtained using the proposed JT1-HC sampling scheme.

7 Conclusions

This paper has presented a comprehensive statistical treatment for analyzing two independent NH lifetime populations under JT1-HC plan. Unlike progressive or accelerated schemes, the JT1-HC design balances cost efficiency and data informativeness by terminating a life test at the earlier of a pre-specified censoring time or a fixed number of failures. We formally established the likelihood structure of this plan and showed its reduction to the joint Type-II censoring design as a limiting case. Within the classical framework, we derived MLEs for the NH scale and shape parameters, along with asymptotic confidence intervals based on the OFI matrix. To overcome the issue of negative lower bounds, we implemented log-transformed intervals, improving reliability in finite samples. On the Bayesian side, we adopted independent gamma priors for all parameters and developed the posterior distribution. Since the conditionals were non-standard, an M–H algorithm was constructed to generate posterior samples, enabling the computation of Bayes point estimators and both equal-tail BCI and HPD interval estimators. Extensive Monte Carlo studies were conducted to evaluate estimator performance under various scenarios of censoring time, failure

percentage, and sample size. The results highlighted several key insights: (i) Bayesian methods, particularly under more informative priors, consistently outperformed classical approaches in terms of RMSE, MAB, and interval precision; (ii) estimator accuracy improved as sample sizes increased and higher percentages of failures were observed; (iii) longer censoring times generally yielded more informative datasets and tighter intervals. Across settings, Bayesian HPD intervals provided the most accurate coverage, while frequentist ACI-NL intervals were most effective for shape parameters and ACI-NA intervals for scale parameters. To demonstrate practical applicability, the proposed methods were applied to three engineering datasets. The NH model provided excellent fits, and analyses of JT1-HC subsamples confirmed the superiority of Bayesian estimators, which produced smaller Std.Es and shorter IWs compared to their frequentist counterparts. Expected mean lifetimes were also reported, offering clear comparisons between groups. The practical implications of the proposed framework are noteworthy in engineering reliability assessment and quality control. Because the NH distribution flexibly captures increasing or decreasing hazard patterns, the JT1-HC approach allows practitioners to analyze incomplete lifetime data for products that do not follow standard exponential assumptions. In industrial settings, this means that comparative life testing can be performed on two production lines simultaneously, reducing both cost and testing time. The obtained reliability and failure rate estimates can directly inform decisions related to maintenance planning, product redesign, and warranty analysis. Consequently, the proposed methodology offers a practical, data-driven tool for engineers and managers seeking to improve system reliability under real-world censoring constraints. The present study can be extended in several directions. First, the proposed framework could be generalized to more than two populations or adapted to progressively joint censoring schemes. Second, future investigations may consider alternative lifetime models or composite distributions that capture additional forms of heterogeneity in engineering reliability data. Moreover, developing analytical and computational strategies for model selection, goodness-of-fit assessment, and Bayesian model averaging under joint censoring scenarios would be of considerable practical interest. Overall, this work contributes a unified likelihood–Bayesian framework for NH models under JT1-HC, introduces computable estimation and interval procedures, provides simulation-based performance guidance, and validates the methodology with real data, thereby equipping practitioners with robust tools for comparative reliability studies.

Acknowledgement: The authors express their gratitude to Princess Nourah bint Abdulrahman University Researchers Supporting Project number (PNURSP2026R50), Princess Nourah bint Abdulrahman University, Riyadh, Saudi Arabia.

Funding Statement: This research was funded by Princess Nourah bint Abdulrahman University Researchers Supporting Project number (PNURSP2026R50), Princess Nourah bint Abdulrahman University, Riyadh, Saudi Arabia.

Author Contributions: The authors confirm contribution to the paper as follows: study conception and design: Refah Alotaibi, Hoda Rezk, Ahmed Elshahhat; data collection: Refah Alotaibi; analysis and interpretation of results: Refah Alotaibi, Ahmed Elshahhat; draft manuscript preparation: Refah Alotaibi, Hoda Rezk, Ahmed Elshahhat. All authors reviewed and approved the final version of the manuscript.

Availability of Data and Materials: The data that support the findings of this study are available within the paper.

Ethics Approval: Not applicable.

Conflicts of Interest: The authors declare no conflicts of interest.

Appendix A The OFI Components

From Eq. (7), the Fisher's items $\mathcal{L}_{ij},\ i,j=1,2$ are:

$$\mathcal{L}_{11}=-\frac{n_1^{\bullet}}{\theta_1^2}-\sum_{i=1}^{n_1^{\bullet}}A_1(w_i)\Big[\log(1+\lambda_1 w_i)\Big]^2-n_1^{\bullet}A_1(\mathcal{T}^{\star})\Big[\log(1+\lambda_1\mathcal{T}^{\star})\Big]^2, \tag{A1}$$

$$\mathcal{L}_{22}=-\frac{n_2^{\bullet}}{\theta_2^2}-\sum_{i=1}^{n_2^{\bullet}}A_2(w_i)\log^2(1+\lambda_2 w_i)-n_2^{\bullet}A_2(\mathcal{T}^{\star})\log^2(1+\lambda_2\mathcal{T}^{\star}), \tag{A2}$$

$$\begin{aligned}\mathcal{L}_{33}=&-\frac{n_1^{\bullet}}{\lambda_1^2}-(\theta_1-1)\sum_{i=1}^{D^{\star}}\frac{w_i^2}{(1+\lambda_1 w_i)^2}\\&-(\theta_1-1)(\theta_1-2)\sum_{i=1}^{n_1^{\bullet}}w_i^2A_1^{\circ\circ}(w_i)-(\theta_1-1)(\theta_1-2)n_1^{\bullet}\mathcal{T}^{\star 2}A_1^{\circ\circ}(\mathcal{T}^{\star}),\end{aligned} \tag{A3}$$

$$\begin{aligned}\mathcal{L}_{44}=&-\frac{n_2^{\bullet}}{\lambda_2^2}-(\theta_2-1)\sum_{i=1}^{D^{\star}}\frac{w_i^2}{(1+\lambda_2 w_i)^2}\\&-(\theta_2-1)(\theta_2-2)\sum_{i=1}^{n_2^{\bullet}}w_i^2A_2^{\circ\circ}(w_i)-n_2^{\bullet}(\theta_2-1)(\theta_2-2)\,\mathcal{T}^{\star 2}A_2^{\circ\circ}(\mathcal{T}^{\star}),\end{aligned} \tag{A4}$$

$$\begin{aligned}\mathcal{L}_{13}=&\sum_{i=1}^{D^{\star}}\frac{w_i}{1+\lambda_1 w_i}-\sum_{i=1}^{n_1^{\bullet}}w_iA_1^{\circ}(w_i)\Big[1+(\theta_1-1)\log(1+\lambda_1 w_i)\Big]\\&-n_1^{\bullet}\mathcal{T}^{\star}A_1^{\circ}(\mathcal{T}^{\star})\Big[1+(\theta_1-1)\log(1+\lambda_1\mathcal{T}^{\star})\Big],\end{aligned} \tag{A5}$$

and

$$\begin{aligned}\mathcal{L}_{24}=&\sum_{i=1}^{D^{\star}}\frac{w_i}{1+\lambda_2 w_i}-\sum_{i=1}^{n_2^{\bullet}}w_iA_2^{\circ}(w_i)\Big[1+(\theta_2-1)\log(1+\lambda_2 w_i)\Big]\\&-n_2^{\bullet}\mathcal{T}^{\star}A_2^{\circ}(\mathcal{T}^{\star})\Big[1+(\theta_2-1)\log(1+\lambda_2\mathcal{T}^{\star})\Big],\end{aligned} \tag{A6}$$

where $A_1^{\circ\circ}(w_i)=(1+\lambda_1 w_i)^{\theta_1-3}$ and $A_2^{\circ\circ}(w_i)=(1+\lambda_2 w_i)^{\theta_2-3}$.

Appendix B Simulation Results

The Monte Carlo simulation results include the point and interval estimation results of θ_i and λ_i (for $i=1,2$).

Table A1: The point estimation outcomes of θ_1.

(n_1, n_2)	FP%	MLE			Bayesian					
					Prior 1			Prior 2		
Set A (at $t^\star$ = 1) →										
(30, 20)	30%	1.175	2.857	1.358	0.447	0.247	0.235	0.382	0.240	0.233
	60%	1.285	2.422	1.145	0.552	0.234	0.225	0.341	0.231	0.220
	90%	0.943	2.104	0.870	0.422	0.229	0.220	0.341	0.224	0.216
(50, 50)	30%	1.510	1.947	0.814	0.372	0.218	0.205	0.267	0.210	0.189
	60%	0.799	1.351	0.757	0.522	0.211	0.203	0.280	0.200	0.183
	90%	0.963	1.048	0.470	0.400	0.210	0.201	0.280	0.195	0.178
(70, 80)	30%	0.875	0.883	0.466	0.510	0.207	0.199	0.397	0.182	0.162
	60%	0.845	0.714	0.387	0.418	0.191	0.181	0.331	0.160	0.151
	90%	0.629	0.442	0.349	0.413	0.163	0.144	0.331	0.157	0.133
Set A (at $t^\star$ = 2) →										
(30, 20)	30%	0.599	2.345	1.310	0.431	0.244	0.234	0.516	0.239	0.226
	60%	0.885	1.965	1.052	0.489	0.233	0.222	0.516	0.227	0.216
	90%	0.511	1.615	0.732	0.415	0.227	0.218	0.435	0.223	0.214
(50, 50)	30%	0.458	1.303	0.731	0.359	0.213	0.205	0.361	0.200	0.183
	60%	0.611	1.066	0.512	0.390	0.211	0.201	0.373	0.195	0.178
	90%	0.353	0.892	0.464	0.404	0.207	0.199	0.395	0.182	0.162
(70, 80)	30%	0.845	0.714	0.387	0.492	0.184	0.174	0.537	0.167	0.147
	60%	0.445	0.667	0.345	0.418	0.173	0.153	0.464	0.154	0.133
	90%	0.629	0.442	0.311	0.413	0.159	0.139	0.463	0.153	0.128
Set B (at $t^\star$ = 0.2) →										
(30, 20)	30%	1.492	3.421	2.487	0.732	0.544	0.543	1.177	0.431	0.419
	60%	1.387	2.224	2.276	0.732	0.484	0.497	0.908	0.426	0.411
	90%	0.875	1.870	2.068	0.732	0.444	0.430	0.977	0.423	0.408
(50, 50)	30%	1.191	1.844	1.922	0.570	0.417	0.405	0.894	0.332	0.306
	60%	1.065	1.450	1.900	0.570	0.403	0.386	0.941	0.319	0.306
	90%	1.265	1.088	1.892	0.570	0.349	0.335	0.994	0.310	0.275
(70, 80)	30%	1.176	0.916	1.884	0.734	0.324	0.309	0.857	0.290	0.259
	60%	1.294	0.908	1.649	0.695	0.305	0.268	0.921	0.263	0.230
	90%	1.239	0.714	1.491	0.695	0.298	0.268	1.121	0.240	0.163
Set B (at $t^\star$ = 0.5) →										
(30, 20)	30%	1.386	2.313	2.375	0.760	0.520	0.426	0.932	0.426	0.406
	60%	1.247	1.935	2.089	0.691	0.443	0.416	0.772	0.420	0.386
	90%	1.373	1.268	1.898	0.665	0.426	0.408	0.742	0.413	0.365
(50, 50)	30%	1.481	1.042	1.681	0.574	0.379	0.345	0.592	0.319	0.340
	60%	1.354	0.991	1.321	0.596	0.357	0.338	0.584	0.312	0.312
	90%	0.985	0.914	1.206	0.589	0.325	0.275	0.581	0.305	0.268
(70, 80)	30%	1.232	0.814	1.173	0.734	0.305	0.268	0.757	0.267	0.231

(Continued)

Table A1 (continued)

(n_1, n_2)	FP%	MLE			Bayesian					
					Prior 1			Prior 2		
	60%	0.981	0.673	0.969	0.614	0.298	0.268	0.674	0.229	0.163
	90%	0.763	0.610	0.860	0.592	0.277	0.241	0.662	0.179	0.149

Table A2: The point estimation outcomes of θ_2.

(n_1, n_2)	FP%	MLE			Bayesian					
					Prior 1			Prior 2		
Set A (at $t^\star = 1$) →										
(30, 20)	30%	1.929	2.477	2.831	1.324	0.445	0.329	1.355	0.411	0.293
	60%	2.015	2.288	2.535	1.298	0.444	0.326	1.334	0.406	0.293
	90%	1.931	2.099	2.141	1.298	0.417	0.290	1.334	0.384	0.279
(50, 50)	30%	1.713	2.005	1.715	1.362	0.403	0.270	1.210	0.351	0.249
	60%	1.562	1.805	1.651	1.370	0.392	0.247	1.209	0.333	0.237
	90%	1.563	1.588	1.359	1.370	0.389	0.246	1.209	0.321	0.222
(70, 80)	30%	1.613	1.484	1.354	1.639	0.379	0.246	1.597	0.309	0.212
	60%	1.610	1.289	1.108	1.557	0.356	0.220	1.519	0.287	0.170
	90%	1.817	1.078	1.045	1.491	0.341	0.215	1.424	0.265	0.126
Set A (at $t^\star = 2$) →										
(30, 20)	30%	1.900	2.358	2.758	1.278	0.432	0.329	1.307	0.399	0.289
	60%	1.636	2.243	2.446	1.237	0.410	0.301	1.310	0.386	0.255
	90%	1.779	2.051	1.934	1.172	0.399	0.280	1.270	0.371	0.249
(50, 50)	30%	1.603	1.933	1.329	1.314	0.399	0.253	1.168	0.343	0.194
	60%	1.400	1.815	1.227	1.316	0.379	0.246	1.175	0.323	0.179
	90%	1.549	1.494	1.172	1.241	0.364	0.227	1.171	0.310	0.159
(70, 80)	30%	1.253	1.395	1.115	1.582	0.364	0.227	1.541	0.298	0.147
	60%	1.581	1.182	1.108	1.557	0.344	0.215	1.519	0.277	0.132
	90%	1.674	1.028	1.045	1.491	0.323	0.212	1.424	0.254	0.126
Set B (at $t^\star = 0.2$) →										
(30, 20)	30%	2.369	2.596	2.944	1.747	0.607	0.535	1.987	0.548	0.437
	60%	2.104	2.333	2.516	1.698	0.598	0.522	1.826	0.528	0.407
	90%	2.104	2.148	2.493	1.698	0.562	0.471	1.873	0.475	0.320
(50, 50)	30%	2.239	2.078	2.441	1.856	0.535	0.320	1.755	0.431	0.286
	60%	1.708	1.795	2.169	1.826	0.518	0.301	1.549	0.414	0.248
	90%	1.708	1.682	1.939	1.860	0.482	0.282	1.691	0.342	0.234
(70, 80)	30%	2.071	1.572	1.794	2.071	0.453	0.255	1.998	0.284	0.229
	60%	1.642	1.395	1.674	2.177	0.434	0.247	1.971	0.277	0.187
	90%	1.842	1.128	1.541	2.048	0.424	0.234	1.911	0.269	0.167

(Continued)

Table A2 (continued)

(n_1, n_2)	FP%	MLE			Bayesian					
					Prior 1			Prior 2		
Set B (at $t^\star$ = 0.5) →										
(30, 20)	30%	2.582	2.770	2.858	1.720	0.550	0.452	1.869	0.475	0.342
	60%	2.325	2.635	2.493	1.598	0.548	0.395	1.710	0.468	0.320
	90%	2.497	2.450	2.148	1.565	0.548	0.345	1.686	0.457	0.303
(50, 50)	30%	2.364	2.271	1.926	1.846	0.457	0.319	1.530	0.374	0.232
	60%	2.249	2.132	1.595	1.828	0.450	0.291	1.478	0.342	0.222
	90%	1.451	1.755	1.433	1.835	0.445	0.281	1.465	0.336	0.217
(70, 80)	30%	2.138	1.654	1.322	2.071	0.424	0.240	1.998	0.277	0.205
	60%	2.117	1.389	1.204	1.987	0.417	0.231	1.991	0.273	0.157
	90%	1.237	1.211	1.192	1.972	0.407	0.221	1.942	0.269	0.113

Table A3: The point estimation outcomes of λ_1.

(n_1, n_2)	FP%	MLE			Bayesian					
					Prior 1			Prior 2		
Set A (at $t^\star$ = 1) →										
(30, 20)	30%	2.176	3.339	3.920	1.337	0.519	0.426	1.291	0.359	0.284
	60%	2.251	3.215	2.559	1.313	0.466	0.366	1.314	0.331	0.254
	90%	2.014	3.011	2.362	1.313	0.426	0.357	1.314	0.323	0.253
(50, 50)	30%	2.345	2.883	2.346	1.308	0.392	0.251	1.255	0.309	0.246
	60%	1.843	2.362	2.285	1.294	0.351	0.242	1.258	0.285	0.229
	90%	1.848	1.856	1.516	1.294	0.320	0.242	1.258	0.269	0.229
(70, 80)	30%	2.257	1.756	1.513	1.314	0.298	0.228	1.144	0.242	0.219
	60%	1.746	1.520	1.215	1.331	0.285	0.228	1.187	0.232	0.196
	90%	2.015	1.317	1.198	1.343	0.278	0.218	1.171	0.222	0.179
Set A (at $t^\star$ = 2) →										
(30, 20)	30%	2.227	3.188	3.781	1.290	0.501	0.411	1.246	0.346	0.274
	60%	1.752	2.782	2.469	1.272	0.466	0.366	1.291	0.323	0.265
	90%	2.056	2.108	2.205	1.328	0.416	0.357	1.337	0.321	0.251
(50, 50)	30%	2.054	2.068	1.762	1.262	0.367	0.251	1.211	0.276	0.237
	60%	1.601	1.851	1.757	1.300	0.341	0.237	1.321	0.272	0.223
	90%	1.919	1.531	1.436	1.314	0.291	0.229	1.278	0.243	0.216
(70, 80)	30%	1.977	1.486	1.382	1.268	0.280	0.221	1.104	0.233	0.211
	60%	1.585	1.200	1.215	1.331	0.278	0.218	1.187	0.222	0.185
	90%	1.828	1.168	1.198	1.343	0.268	0.210	1.171	0.186	0.167
Set B (at $t^\star$ = 0.2) →										
(30, 20)	30%	2.568	3.098	3.553	1.888	0.645	0.554	1.896	0.485	0.392

(Continued)

Table A3 (continued)

(n_1, n_2)	FP%	MLE			Bayesian					
					Prior 1			Prior 2		
	60%	2.439	2.930	3.246	1.770	0.625	0.539	1.851	0.446	0.392
	90%	2.587	2.786	3.246	1.828	0.607	0.518	1.751	0.416	0.359
(50, 50)	30%	2.325	2.409	2.235	1.757	0.415	0.364	1.694	0.391	0.335
	60%	2.265	2.290	2.072	1.669	0.410	0.358	1.754	0.388	0.329
	90%	2.265	2.137	2.072	1.694	0.391	0.346	1.644	0.378	0.312
(70, 80)	30%	2.083	2.073	1.916	1.721	0.386	0.329	1.541	0.364	0.286
	60%	2.055	1.990	1.799	1.689	0.363	0.321	1.575	0.341	0.263
	90%	1.859	1.814	1.599	1.619	0.346	0.262	1.517	0.319	0.256
Set B (at $t^\star$ = 0.5) →										
(30, 20)	30%	1.867	1.958	3.265	1.798	0.625	0.539	1.745	0.433	0.373
	60%	2.030	1.917	2.193	1.695	0.617	0.523	1.663	0.421	0.361
	90%	2.268	1.176	1.772	1.685	0.607	0.518	1.636	0.415	0.359
(50, 50)	30%	2.830	0.901	1.415	1.690	0.393	0.356	1.642	0.382	0.321
	60%	1.692	0.836	1.386	1.627	0.391	0.356	1.671	0.378	0.311
	90%	1.948	0.760	1.132	1.639	0.387	0.338	1.680	0.366	0.309
(70, 80)	30%	2.414	0.679	1.036	1.721	0.361	0.314	1.541	0.328	0.273
	60%	1.714	0.569	0.964	1.734	0.359	0.302	1.502	0.318	0.253
	90%	1.883	0.440	0.919	1.767	0.334	0.259	1.524	0.308	0.233

Table A4: The point estimation outcomes of λ_2.

(n_1, n_2)	FP%	MLE			Bayesian					
					Prior 1			Prior 2		
Set A (at $t^\star$ = 1) →										
(30, 20)	30%	1.297	2.173	1.368	0.436	0.533	0.454	0.419	0.373	0.347
	60%	1.153	1.872	1.259	0.466	0.422	0.417	0.447	0.351	0.332
	90%	1.181	1.767	1.180	0.452	0.396	0.375	0.423	0.349	0.321
(50, 50)	30%	0.885	1.555	0.874	0.491	0.388	0.353	0.462	0.323	0.313
	60%	0.852	1.257	0.835	0.523	0.360	0.333	0.548	0.322	0.302
	90%	0.858	1.178	0.805	0.511	0.334	0.326	0.472	0.309	0.296
(70, 80)	30%	0.723	1.064	0.679	0.457	0.319	0.310	0.409	0.301	0.285
	60%	0.780	0.924	0.664	0.405	0.308	0.305	0.325	0.279	0.254
	90%	1.256	0.789	0.534	0.498	0.283	0.287	0.497	0.237	0.239
Set A (at $t^\star$ = 2) →										
(30, 20)	30%	1.610	1.725	1.247	0.242	0.420	0.354	0.270	0.351	0.359
	60%	0.969	1.472	1.033	0.264	0.404	0.343	0.280	0.345	0.331
	90%	1.313	1.045	0.888	0.241	0.382	0.329	0.244	0.337	0.311

(Continued)

Table A4 (continued)

(n_1, n_2)	FP%	MLE			Bayesian					
					Prior 1			Prior 2		
(50, 50)	30%	0.854	1.000	0.865	0.263	0.360	0.328	0.297	0.322	0.307
	60%	0.797	0.891	0.805	0.275	0.343	0.321	0.291	0.301	0.296
	90%	1.289	0.891	0.684	0.273	0.334	0.312	0.263	0.284	0.260
(70, 80)	30%	0.697	0.595	0.641	0.245	0.318	0.301	0.263	0.279	0.254
	60%	0.780	0.595	0.614	0.225	0.302	0.292	0.217	0.274	0.245
	90%	1.256	0.294	0.534	0.207	0.245	0.277	0.198	0.231	0.227
Set B (at $t^\star$ = 0.2) →										
(30, 20)	30%	1.768	2.340	2.471	1.354	0.633	0.761	1.240	0.540	0.527
	60%	1.514	2.203	2.257	1.274	0.633	0.681	1.318	0.517	0.504
	90%	1.428	2.164	2.129	1.286	0.633	0.621	1.430	0.493	0.472
(50, 50)	30%	1.202	2.088	2.055	1.236	0.593	0.583	1.545	0.475	0.451
	60%	1.314	1.940	1.985	1.225	0.570	0.559	1.408	0.450	0.417
	90%	1.324	1.155	1.848	1.355	0.536	0.515	1.355	0.421	0.390
(70, 80)	30%	1.063	1.133	1.791	1.296	0.446	0.424	1.160	0.389	0.345
	60%	1.131	0.947	1.575	1.149	0.425	0.400	1.234	0.369	0.334
	90%	1.245	0.908	1.257	1.217	0.369	0.345	1.144	0.352	0.322
Set B (at $t^\star$ = 0.5) →										
(30, 20)	30%	1.851	2.376	2.731	1.286	0.618	0.596	0.955	0.456	0.442
	60%	1.677	2.258	2.113	1.135	0.607	0.593	0.903	0.426	0.408
	90%	1.482	2.159	2.022	1.091	0.601	0.586	0.871	0.392	0.383
(50, 50)	30%	1.726	1.831	1.994	0.975	0.536	0.515	1.045	0.389	0.377
	60%	1.641	1.422	1.758	0.888	0.524	0.506	1.001	0.360	0.364
	90%	1.987	1.206	1.466	0.875	0.484	0.474	0.983	0.341	0.320
(70, 80)	30%	1.804	1.106	1.338	0.910	0.450	0.385	0.885	0.326	0.313
	60%	1.586	1.064	1.253	0.828	0.390	0.371	0.927	0.315	0.301
	90%	1.355	0.789	1.202	0.991	0.372	0.336	0.979	0.309	0.280

Table A5: The interval estimation outcomes of θ_1.

(n, m)	FP%	ACI-NA		ACI-NL		BCI				HPD			
						Prior-1		Prior-2		Prior-1		Prior-2	
Set A (at $t^\star$ = 1) →													
(30, 20)	30%	0.986	0.956	0.915	0.958	0.493	0.972	0.454	0.973	0.343	0.977	0.331	0.977
	60%	0.824	0.961	0.589	0.969	0.426	0.974	0.392	0.975	0.295	0.978	0.282	0.979
	90%	0.758	0.964	0.452	0.973	0.396	0.975	0.365	0.976	0.295	0.978	0.274	0.979
(50, 50)	30%	0.708	0.965	0.369	0.976	0.342	0.977	0.314	0.979	0.280	0.979	0.273	0.979
	60%	0.519	0.971	0.359	0.976	0.319	0.978	0.294	0.979	0.261	0.980	0.236	0.980

(Continued)

Table A5 (continued)

(n, m)	FP%	ACI-NA		ACI-NL		BCI				HPD			
						Prior-1		Prior-2		Prior-1		Prior-2	
	90%	0.500	0.972	0.345	0.977	0.267	0.979	0.246	0.980	0.249	0.980	0.220	0.981
(70, 80)	30%	0.496	0.972	0.234	0.980	0.227	0.981	0.209	0.981	0.213	0.981	0.174	0.982
	60%	0.364	0.976	0.223	0.981	0.216	0.981	0.199	0.981	0.205	0.981	0.167	0.983
	90%	0.350	0.977	0.219	0.981	0.216	0.981	0.199	0.982	0.197	0.982	0.125	0.984
Set A (at $t^\star = 2$) →													
(30, 20)	30%	0.865	0.960	0.702	0.959	0.485	0.972	0.471	0.973	0.333	0.977	0.321	0.978
	60%	0.608	0.968	0.504	0.972	0.415	0.975	0.402	0.975	0.291	0.979	0.278	0.979
	90%	0.465	0.973	0.451	0.973	0.383	0.976	0.369	0.976	0.291	0.979	0.272	0.979
(50, 50)	30%	0.383	0.976	0.358	0.976	0.334	0.977	0.283	0.979	0.280	0.979	0.267	0.979
	60%	0.350	0.977	0.322	0.978	0.313	0.978	0.267	0.979	0.243	0.980	0.230	0.981
	90%	0.350	0.977	0.295	0.978	0.261	0.980	0.257	0.980	0.224	0.981	0.216	0.981
(70, 80)	30%	0.291	0.979	0.231	0.981	0.227	0.981	0.217	0.981	0.211	0.981	0.170	0.983
	60%	0.252	0.980	0.222	0.981	0.210	0.981	0.205	0.981	0.188	0.982	0.160	0.983
	90%	0.221	0.981	0.216	0.981	0.210	0.981	0.199	0.982	0.182	0.982	0.124	0.984
Set B (at $t^\star = 0.2$) →													
(30, 20)	30%	1.893	0.927	1.803	0.930	0.629	0.968	0.578	0.968	0.500	0.972	0.491	0.972
	60%	1.756	0.931	1.495	0.940	0.618	0.968	0.568	0.968	0.495	0.972	0.451	0.973
	90%	1.624	0.936	1.279	0.947	0.613	0.968	0.564	0.969	0.495	0.972	0.445	0.974
(50, 50)	30%	1.524	0.939	0.714	0.965	0.592	0.969	0.545	0.969	0.464	0.973	0.429	0.974
	60%	1.455	0.941	0.698	0.966	0.519	0.971	0.477	0.973	0.463	0.973	0.418	0.975
	90%	1.246	0.948	0.660	0.967	0.484	0.972	0.445	0.973	0.438	0.974	0.381	0.976
(70, 80)	30%	1.025	0.955	0.575	0.969	0.460	0.973	0.423	0.974	0.376	0.976	0.353	0.977
	60%	0.971	0.957	0.497	0.972	0.442	0.974	0.407	0.976	0.358	0.976	0.320	0.978
	90%	0.927	0.958	0.475	0.973	0.423	0.974	0.389	0.976	0.350	0.977	0.241	0.980
Set B (at $t^\star = 0.5$) →													
(30, 20)	30%	1.842	0.929	1.770	0.931	0.629	0.968	0.624	0.968	0.500	0.972	0.491	0.972
	60%	1.617	0.936	1.487	0.940	0.613	0.968	0.607	0.968	0.483	0.972	0.444	0.974
	90%	1.524	0.939	1.201	0.949	0.608	0.968	0.581	0.969	0.483	0.972	0.437	0.974
(50, 50)	30%	1.279	0.947	0.698	0.966	0.581	0.969	0.573	0.970	0.463	0.973	0.413	0.975
	60%	1.210	0.949	0.626	0.968	0.478	0.973	0.464	0.973	0.420	0.974	0.391	0.975
	90%	0.984	0.956	0.592	0.969	0.476	0.973	0.463	0.973	0.419	0.974	0.368	0.976
(70, 80)	30%	0.918	0.958	0.547	0.970	0.448	0.974	0.397	0.975	0.363	0.976	0.338	0.977
	60%	0.857	0.960	0.492	0.972	0.397	0.975	0.365	0.976	0.354	0.977	0.242	0.980
	90%	0.809	0.962	0.466	0.973	0.397	0.975	0.358	0.976	0.348	0.977	0.234	0.980

Table A6: The interval estimation outcomes of θ_2.

(n, m)	FP%	ACI-NA		ACI-NL		BCI				HPD			
						Prior-1		Prior-2		Prior-1		Prior-2	
Set A (at $t^\star = 1$) →													
(30, 20)	30%	1.654	0.947	1.369	0.952	1.302	0.954	1.211	0.960	0.929	0.961	0.905	0.961
	60%	1.521	0.949	1.344	0.953	1.298	0.954	1.207	0.961	0.873	0.962	0.786	0.964
	90%	1.384	0.953	1.282	0.954	0.926	0.961	0.861	0.962	0.673	0.966	0.604	0.967
(50, 50)	30%	1.359	0.953	1.269	0.954	0.913	0.961	0.849	0.962	0.653	0.966	0.527	0.969
	60%	1.300	0.954	1.211	0.955	0.891	0.962	0.829	0.963	0.577	0.968	0.514	0.970
	90%	1.300	0.954	1.096	0.958	0.831	0.963	0.773	0.963	0.418	0.971	0.355	0.970
(70, 80)	30%	1.016	0.959	0.983	0.960	0.812	0.963	0.755	0.964	0.403	0.971	0.349	0.971
	60%	0.993	0.960	0.957	0.960	0.803	0.963	0.747	0.964	0.357	0.973	0.209	0.974
	90%	0.983	0.960	0.937	0.960	0.753	0.964	0.700	0.965	0.311	0.973	0.196	0.976
Set A (at $t^\star = 2$) →													
(30, 20)	30%	1.208	0.949	1.328	0.953	1.263	0.954	0.951	0.961	0.923	0.961	0.877	0.962
	60%	1.204	0.953	1.303	0.954	1.233	0.955	0.925	0.961	0.847	0.963	0.682	0.966
	90%	0.859	0.954	1.231	0.955	0.903	0.961	0.847	0.963	0.666	0.966	0.586	0.968
(50, 50)	30%	0.847	0.954	1.212	0.955	0.877	0.962	0.818	0.963	0.603	0.967	0.470	0.970
	60%	0.826	0.955	1.145	0.957	0.869	0.962	0.813	0.963	0.519	0.969	0.323	0.973
	90%	0.771	0.957	1.032	0.959	0.829	0.963	0.785	0.964	0.374	0.972	0.317	0.973
(70, 80)	30%	0.753	0.960	0.961	0.960	0.810	0.963	0.762	0.964	0.364	0.972	0.288	0.973
	60%	0.745	0.960	0.953	0.960	0.779	0.964	0.730	0.965	0.295	0.973	0.203	0.975
	90%	0.698	0.960	0.933	0.961	0.732	0.965	0.670	0.966	0.200	0.975	0.188	0.976
Set B (at $t^\star = 0.2$) →													
(30, 20)	30%	2.470	0.931	2.219	0.936	1.660	0.947	1.543	0.950	1.296	0.954	1.001	0.960
	60%	2.239	0.935	2.054	0.939	1.496	0.950	1.391	0.952	1.169	0.956	0.995	0.960
	90%	2.187	0.937	1.914	0.942	1.444	0.951	1.343	0.952	1.122	0.957	0.979	0.960
(50, 50)	30%	2.015	0.940	1.498	0.950	1.395	0.952	1.298	0.953	1.020	0.959	0.918	0.961
	60%	1.987	0.940	1.380	0.952	1.297	0.954	1.206	0.957	0.938	0.961	0.886	0.962
	90%	1.622	0.947	1.317	0.953	1.268	0.954	1.179	0.961	0.910	0.961	0.728	0.965
(70, 80)	30%	1.424	0.951	1.259	0.955	1.208	0.956	1.124	0.961	0.862	0.962	0.519	0.969
	60%	1.268	0.954	1.195	0.956	1.136	0.957	1.056	0.962	0.854	0.962	0.446	0.970
	90%	1.177	0.959	1.150	0.957	1.109	0.957	1.031	0.963	0.758	0.964	0.357	0.972
Set B (at $t^\star = 0.5$) →													
(30, 20)	30%	1.539	0.935	2.024	0.940	1.487	0.950	1.389	0.952	1.042	0.959	0.981	0.960
	60%	1.388	0.937	1.821	0.944	1.440	0.951	1.355	0.953	1.010	0.959	0.941	0.961
	90%	1.339	0.938	1.742	0.945	1.420	0.951	1.337	0.953	0.995	0.960	0.923	0.963
(50, 50)	30%	1.294	0.942	1.395	0.952	1.357	0.953	1.057	0.958	0.979	0.960	0.908	0.963
	60%	1.203	0.942	1.314	0.953	1.280	0.954	0.945	0.961	0.918	0.961	0.630	0.967
	90%	1.176	0.949	1.286	0.954	1.229	0.955	0.918	0.961	0.880	0.962	0.586	0.968

(Continued)

Table A6 (continued)

(n, m)	FP%	ACI-NA		ACI-NL		BCI				HPD			
						Prior-1		Prior-2		Prior-1		Prior-2	
(70, 80)	30%	1.121	0.954	1.229	0.955	1.175	0.956	0.892	0.962	0.854	0.962	0.470	0.970
	60%	1.053	0.955	1.162	0.956	1.124	0.957	0.888	0.962	0.841	0.963	0.430	0.971
	90%	1.029	0.957	1.125	0.957	0.860	0.962	0.803	0.963	0.620	0.967	0.350	0.972

Table A7: The interval estimation outcomes of λ_1.

(n, m)	FP%	ACI-NA		ACI-NL		BCI				HPD			
						Prior-1		Prior-2		Prior-1		Prior-2	
Set A (at $t^\star = 1$) →													
(30, 20)	30%	1.179	0.959	1.226	0.958	1.117	0.961	1.064	0.962	0.971	0.964	0.918	0.965
	60%	1.096	0.961	1.182	0.959	0.946	0.965	0.896	0.966	0.814	0.968	0.781	0.969
	90%	0.994	0.964	1.124	0.961	0.940	0.965	0.843	0.967	0.802	0.968	0.646	0.972
(50, 50)	30%	0.840	0.967	0.935	0.965	0.800	0.968	0.654	0.972	0.555	0.974	0.529	0.975
	60%	0.834	0.967	0.869	0.967	0.799	0.968	0.546	0.974	0.513	0.975	0.460	0.976
	90%	0.794	0.968	0.829	0.968	0.744	0.970	0.518	0.975	0.383	0.978	0.354	0.979
(70, 80)	30%	0.781	0.969	0.799	0.968	0.653	0.972	0.457	0.976	0.343	0.979	0.314	0.980
	60%	0.770	0.969	0.796	0.968	0.572	0.974	0.415	0.977	0.341	0.979	0.263	0.981
	90%	0.725	0.970	0.796	0.968	0.540	0.974	0.319	0.980	0.252	0.981	0.239	0.981
Set A (at $t^\star = 2$) →													
(30, 20)	30%	1.144	0.960	1.189	0.959	1.079	0.962	1.001	0.964	0.942	0.965	0.859	0.967
	60%	1.081	0.962	1.134	0.960	0.904	0.966	0.861	0.967	0.809	0.968	0.674	0.971
	90%	0.962	0.964	1.018	0.963	0.896	0.966	0.834	0.967	0.777	0.969	0.521	0.975
(50, 50)	30%	0.822	0.968	0.849	0.967	0.695	0.971	0.577	0.973	0.551	0.974	0.500	0.975
	60%	0.822	0.968	0.849	0.967	0.563	0.974	0.544	0.974	0.474	0.976	0.378	0.978
	90%	0.787	0.969	0.806	0.968	0.538	0.974	0.515	0.975	0.377	0.978	0.329	0.979
(70, 80)	30%	0.755	0.969	0.787	0.969	0.531	0.975	0.432	0.977	0.342	0.979	0.283	0.980
	60%	0.747	0.970	0.775	0.969	0.425	0.977	0.403	0.978	0.282	0.980	0.251	0.981
	90%	0.707	0.970	0.756	0.969	0.341	0.979	0.297	0.980	0.250	0.981	0.213	0.982
Set B (at $t^\star = 0.2$) →													
(30, 20)	30%	1.596	0.950	2.177	0.936	1.325	0.956	1.278	0.957	1.218	0.958	0.983	0.964
	60%	1.474	0.952	1.925	0.942	1.284	0.957	1.237	0.958	1.138	0.960	0.972	0.964
	90%	1.274	0.957	1.725	0.947	1.204	0.959	1.099	0.961	1.018	0.963	0.923	0.965
(50, 50)	30%	1.065	0.962	1.602	0.949	0.981	0.964	0.958	0.965	0.916	0.966	0.591	0.973
	60%	0.979	0.964	1.549	0.951	0.964	0.964	0.926	0.965	0.800	0.968	0.582	0.973
	90%	0.920	0.965	1.349	0.955	0.909	0.966	0.881	0.966	0.759	0.969	0.516	0.975
(70, 80)	30%	0.893	0.966	0.974	0.964	0.775	0.969	0.688	0.971	0.496	0.975	0.476	0.976

(Continued)

Table A7 (continued)

(n, m)	FP%	ACI-NA		ACI-NL		BCI				HPD			
						Prior-1		Prior-2		Prior-1		Prior-2	
	60%	0.789	0.969	0.854	0.967	0.711	0.970	0.573	0.974	0.471	0.976	0.366	0.978
	90%	0.739	0.970	0.810	0.968	0.456	0.976	0.451	0.976	0.432	0.977	0.362	0.979
Set B (at $t^\star$ = 0.5) →													
(30, 20)	30%	1.339	0.956	2.090	0.938	1.284	0.957	1.240	0.958	1.208	0.959	0.981	0.964
	60%	1.319	0.956	1.762	0.946	1.240	0.958	1.180	0.959	1.094	0.961	0.931	0.965
	90%	1.233	0.958	1.468	0.953	1.172	0.960	1.031	0.963	0.964	0.964	0.859	0.967
(50, 50)	30%	0.981	0.964	1.341	0.956	0.970	0.964	0.957	0.965	0.802	0.968	0.589	0.973
	60%	0.966	0.964	1.175	0.959	0.932	0.965	0.881	0.966	0.785	0.969	0.575	0.974
	90%	0.917	0.966	1.175	0.959	0.889	0.966	0.877	0.966	0.580	0.973	0.487	0.976
(70, 80)	30%	0.874	0.967	0.896	0.966	0.741	0.970	0.632	0.972	0.478	0.976	0.452	0.976
	60%	0.748	0.969	0.796	0.968	0.576	0.974	0.539	0.974	0.458	0.976	0.354	0.979
	90%	0.706	0.970	0.740	0.970	0.455	0.976	0.433	0.977	0.391	0.978	0.348	0.979

Table A8: The interval estimation outcomes of λ_2.

(n, m)	FP%	ACI-NA		ACI-NL		BCI				HPD			
						Prior-1		Prior-2		Prior-1		Prior-2	
Set A (at $t^\star$ = 1) →													
(30, 20)	30%	0.890	0.968	1.771	0.946	0.862	0.969	0.785	0.971	0.760	0.971	0.683	0.973
	60%	0.876	0.968	1.435	0.954	0.818	0.970	0.776	0.971	0.744	0.972	0.671	0.973
	90%	0.854	0.969	1.331	0.957	0.805	0.970	0.745	0.972	0.733	0.972	0.671	0.973
(50, 50)	30%	0.778	0.971	1.230	0.960	0.674	0.973	0.605	0.975	0.595	0.975	0.548	0.976
	60%	0.651	0.974	1.126	0.962	0.636	0.974	0.580	0.976	0.575	0.976	0.528	0.977
	90%	0.642	0.974	0.871	0.968	0.621	0.975	0.580	0.976	0.516	0.977	0.508	0.977
(70, 80)	30%	0.510	0.977	0.671	0.973	0.452	0.979	0.396	0.980	0.341	0.982	0.279	0.983
	60%	0.473	0.978	0.553	0.976	0.429	0.979	0.370	0.981	0.306	0.982	0.271	0.983
	90%	0.443	0.979	0.469	0.978	0.410	0.980	0.355	0.981	0.279	0.983	0.264	0.983
Set A (at $t^\star$ = 2) →													
(30, 20)	30%	0.887	0.968	1.538	0.952	0.839	0.969	0.771	0.971	0.737	0.972	0.662	0.974
	60%	0.862	0.969	1.347	0.957	0.792	0.970	0.771	0.971	0.715	0.972	0.647	0.974
	90%	0.828	0.970	1.118	0.962	0.768	0.971	0.744	0.972	0.692	0.973	0.621	0.975
(50, 50)	30%	0.724	0.972	1.025	0.965	0.656	0.974	0.596	0.975	0.593	0.975	0.538	0.977
	60%	0.640	0.974	0.723	0.972	0.590	0.975	0.577	0.976	0.531	0.977	0.457	0.979
	90%	0.637	0.974	0.651	0.974	0.590	0.975	0.565	0.976	0.528	0.977	0.454	0.979
(70, 80)	30%	0.473	0.978	0.537	0.977	0.429	0.979	0.373	0.981	0.295	0.983	0.272	0.983
	60%	0.436	0.979	0.486	0.978	0.425	0.979	0.315	0.982	0.285	0.983	0.264	0.983
	90%	0.423	0.980	0.456	0.979	0.402	0.980	0.302	0.983	0.276	0.983	0.253	0.984

(Continued)

Table A8 (continued)

(n, m)	FP%	ACI-NA		ACI-NL		BCI				HPD			
						Prior-1		Prior-2		Prior-1		Prior-2	
Set B (at $t^\star$ = 0.2) →													
(30, 20)	30%	1.186	0.961	2.466	0.929	1.074	0.963	0.992	0.965	0.990	0.966	0.933	0.967
	60%	1.149	0.962	2.295	0.933	1.074	0.963	0.991	0.965	0.954	0.966	0.897	0.968
	90%	1.088	0.963	2.074	0.939	1.074	0.963	0.991	0.965	0.945	0.967	0.887	0.968
(50, 50)	30%	1.061	0.964	1.895	0.943	0.860	0.969	0.821	0.970	0.745	0.972	0.703	0.973
	60%	1.010	0.965	1.700	0.948	0.835	0.969	0.821	0.970	0.744	0.972	0.702	0.973
	90%	0.860	0.969	1.743	0.947	0.821	0.970	0.809	0.970	0.733	0.972	0.696	0.973
(70, 80)	30%	0.767	0.971	1.555	0.952	0.734	0.972	0.697	0.973	0.400	0.980	0.392	0.980
	60%	0.697	0.973	1.255	0.959	0.642	0.974	0.525	0.977	0.387	0.980	0.377	0.981
	90%	0.674	0.973	1.108	0.963	0.636	0.974	0.502	0.978	0.387	0.980	0.374	0.981
Set B (at $t^\star$ = 0.5) →													
(30, 20)	30%	1.178	0.961	2.339	0.932	1.061	0.964	0.991	0.965	0.979	0.966	0.933	0.967
	60%	1.095	0.963	2.287	0.933	0.992	0.965	0.980	0.966	0.933	0.967	0.893	0.968
	90%	1.078	0.963	2.041	0.940	0.992	0.965	0.971	0.966	0.933	0.967	0.882	0.968
(50, 50)	30%	1.010	0.965	1.862	0.944	0.854	0.969	0.817	0.970	0.733	0.972	0.696	0.973
	60%	0.860	0.969	1.166	0.961	0.822	0.970	0.779	0.971	0.733	0.972	0.696	0.973
	90%	0.850	0.969	0.982	0.966	0.814	0.970	0.763	0.971	0.723	0.972	0.681	0.973
(70, 80)	30%	0.734	0.972	0.938	0.967	0.697	0.973	0.678	0.973	0.400	0.980	0.392	0.980
	60%	0.664	0.974	0.831	0.969	0.599	0.975	0.499	0.978	0.383	0.981	0.361	0.980
	90%	0.642	0.974	0.765	0.971	0.576	0.976	0.429	0.979	0.378	0.981	0.355	0.981

References

1. Balakrishnan N, Kundu D. Hybrid censoring: models, inferential results and applications. Comput Stat Data Anal. 2013;57(1):166–209. doi:10.1016/j.csda.2012.03.025.
2. Epstein B. Truncated life tests in the exponential case. Ann Math Statist. 1954;25(3):555–64. doi:10.1214/aoms/1177728723.
3. Childs A, Chandrasekar B, Balakrishnan N, Kundu D. Exact likelihood inference based on type-I and type-II hybrid censored samples from the exponential distribution. Ann Inst Stat Math. 2003;55(2):319–30. doi:10.1007/bf02530502.
4. Balakrishnan N, Rasouli A. Exact likelihood inference for two exponential populations under joint type-II censoring. Comput Stat Data Anal. 2008;52(5):2725–38. doi:10.1016/j.csda.2007.10.005.
5. Su F. Exact likelihood inference for multiple exponential populations under joint censoring [master's thesis]. Hamilton, ON, Canada: McMaster University; 2013.
6. Su F, Zhu X. Exact likelihood inference for two exponential populations based on a joint generalized type-I hybrid censored sample. J Stat Comput Simul. 2016;86(7):1342–62. doi:10.1080/00949655.2015.1062483.
7. Rasouli A, Balakrishnan N. Exact likelihood inference for two exponential populations under joint progressive type-II censoring. Commun Stat Theory Methods. 2010;39(12):2172–91. doi:10.1080/03610920903009418.
8. Sultana F, Çetinkaya Ç, Kundu D. Statistical inference for the jointly adaptive progressive type-II censored weibull distributions. J Stat Theory Pract. 2023;17(2):24. doi:10.1007/s42519-022-00318-z.

9. Elshahhat A, Ahmad HH, Rabaiah A, Abo-Kasem OE. Analysis of a new jointly hybrid censored Rayleigh populations. AIMS Math. 2024;9(2):3740–62. doi:10.3934/math.2024184.
10. Nadarajah S, Haghighi F. An extension of the exponential distribution. Statistics. 2011;45(6):543–58. doi:10.1080/02331881003678678.
11. Kumar D, Dey S, Nadarajah S. Extended exponential distribution based on order statistics. Commun Stat Theory Methods. 2017;46(18):9166–84. doi:10.1080/03610926.2016.1205625.
12. Kumar D, Malik MR, Dey S, Shahbaz MQ. Recurrence relations for moments and estimation of parameters of extended exponential distribution based on progressive type-II right-censored order statistics. J Stat Theory Appl. 2019;18(2):171–81. doi:10.2991/jsta.d.190514.003.
13. Ashour SK, El-Sheikh AA, Elshahhat A. Inferences and optimal censoring schemes for progressively first-failure censored Nadarajah-Haghighi distribution. Sankhya A. 2022;84(2):885–923. doi:10.1007/s13171-019-00175-2.
14. Elbatal I, Alotaibi N, Alyami SA, Elgarhy M, El-Saeed AR. Bayesian and non-Bayesian estimation of the Nadarajah-Haghighi distribution: using progressive type-1 censoring scheme. Mathematics. 2022;10(5):760. doi:10.3390/math10050760.
15. Wu M, Gui W. Estimation and prediction for Nadarajah-Haghighi distribution under progressive type-II censoring. Symmetry. 2021;13(6):999. doi:10.3390/sym13060999.
16. Elshahhat A, Abu El Azm WS. Statistical reliability analysis of electronic devices using generalized progressively hybrid censoring plan. Qual Reliab Eng Int. 2022;38(2):1112–30. doi:10.1002/qre.3058.
17. Dey S, Wang L, Nassar M. Inference on Nadarajah-Haghighi distribution with constant stress partially accelerated life tests under progressive type-II censoring. J Appl Stat. 2022;49(11):2891–912. doi:10.1080/02664763.2021.1928014.
18. Almarashi AM, Algarni A, Okasha H, Nassar M. On reliability estimation of Nadarajah-Haghighi distribution under adaptive type-I progressive hybrid censoring scheme. Qual Reliab Eng Int. 2022;38(2):817–33. doi:10.1002/qre.3016.
19. Elshahhat A, Alotaibi R, Nassar M. Inferences for Nadarajah-Haghighi parameters via type-II adaptive progressive hybrid censoring with applications. Mathematics. 2022;10(20):3775. doi:10.3390/math10203775.
20. Hasaballah MM, Tashkandy YA, Balogun OS, Bakr ME. Reliability analysis for two populations Nadarajah-Haghighi distribution under joint progressive type-II censoring. AIMS Math. 2024;9(4):10333–52. doi:10.3934/math.2024505.
21. El-Sherpieny ESA, Elshahhat A, Abdallah NM. Statistical analysis of improved type-II adaptive progressive hybrid censored NH data. Sankhya A. 2024;86(2):721–54. doi:10.1007/s13171-024-00345-x.
22. Henningsen A, Toomet O. maxLik: a package for maximum likelihood estimation in R. Comput Stat. 2011;26(3):443–58. doi:10.1007/s00180-010-0217-1.
23. Lawless JF. Statistical models and methods for lifetime data. New York, NY, USA: John Wiley and Sons; 2011. doi:10.1002/9781118033005.
24. Meeker WQ, Escobar LA. Statistical methods for reliability data. New York, NY, USA: John Wiley and Sons; 1998. doi:10.2307/1271181.
25. Kundu D. Bayesian inference and life testing plan for the Weibull distribution in presence of progressive censoring. Technometrics. 2008;50(2):144–54. doi:10.1198/004017008000000217.
26. Bayoud HA, Raqab MZ. Classical and Bayesian inferences for two Topp-Leone models under joint progressive type-II censoring. Commun Stat Simul Comput. 2024;53(1):427–45. doi:10.1080/03610918.2021.2023180.
27. Alqasem OA, Mohammed HS, Elshahhat A, Hussein HA, Jaheen ZF. Bayesian and empirical-Bayesian evaluations of the Topp-Leone lifetime model using lower record statistics. AIP Adv. 2024;14(4):045124. doi:10.1063/5.0176939.
28. Murthy DNP, Xie M, Jiang R. Weibull models. In: Wiley series in probability and statistics. Hoboken, NJ, USA: Wiley; 2004. doi:10.1002/047147326x.
29. Proschan F. Theoretical explanation of observed decreasing failure rate. Technometrics. 1963;5(3):375–83. doi:10.2307/1266340.
30. Abo-Kasem OE, Elshahhat A. Analysis of two Weibull populations under joint progressively hybrid censoring. Commun Stat Simul Comput. 2023;52(9):4469–90. doi:10.1080/03610918.2021.1963452.

31. Bagdonavicius V, Nikulin M. Accelerated life models: modeling and statistical analysis. Boca Raton, FL, USA: Chapman and Hall/CRC; 2001. doi:10.1201/9781420035872.
32. Peng X, Yan Z. Estimation and application for a new extended Weibull distribution. Reliab Eng Syst Saf. 2014;121(2):34–42. doi:10.1016/j.ress.2013.07.007.
33. Pinho LGB, Cordeiro GM, Nobre JS. The Harris extended exponential distribution. Commun Stat Theory Methods. 2015;44(16):3486–502. doi:10.1080/03610926.2013.851221.
34. Mahdavi A, Kundu D. A new method for generating distributions with an application to exponential distribution. Commun Stat Theory Methods. 2017;46(13):6543–57. doi:10.1080/03610926.2015.1130839.
35. Birnbaum ZW, Saunders SC. A probabilistic interpretation of Miner's rule. SIAM J Appl Math. 1968;16(3):637–52. doi:10.1137/0116052.
36. Marinho PRD, Silva RB, Bourguignon M, Cordeiro GM, Nadarajah S. An R package for probability distributions and general purpose optimization. PLoS One. 2019;14(8):e0221487. doi:10.1371/journal.pone.0221487.